solids

MDPI

Review

Sustainable Approaches to Incorporate Plant-Based Biomaterials in Power Generation

Antonio Ruiz-Gonzalez [1,*], Mingqing Wang [2] and Jim Haseloff [1]

[1] Department of Plant Sciences, University of Cambridge, Downing St., Cambridge CB2 3EA, UK
[2] Institute for Materials Discovery, Faculty of Mathematical & Physical Sciences, University College London, 107 Roberts Building, Malet Place, London WC1E 7JE, UK; mingqing.wang@ucl.ac.uk
* Correspondence: a.gonzalez.16@ucl.ac.uk

Abstract: Biomass-derived materials have traditionally been used to generate electrical energy through the combustion of their organic components. However, within the past few years, certain common biomass compounds, especially plant-based products such as cellulose and lignin, have drawn attention in the energy field due to their wide availability, low cost, and chemical versatility. In the case of cellulose, the combination of crystalline and amorphous domains, along with the high surface area and abundance of hydroxyl groups, has allowed for its application in multiple devices to harvest energy from the environment. However, to date, there are no reviews focusing on the different approaches that have been developed to implement these sustainable materials in the generation of renewable energies and the desirable material properties for these applications. This manuscript reviews alternative ways that have been developed to exploit biomass compounds in power generation, especially cellulose and lignin. Three different types of energy harvesting are discussed: mechanical, osmotic, and thermal energy. In the case of mechanical energy, the application of plant-derived materials in piezoelectric and triboelectric generators is described. In both cases, approaches where the biomass material has an active role in power generation instead of acting as a mechanical support are reported. For osmotic energy, the performance of inverse electrodialysis systems and the use of plant-derived materials, including the chemical modifications carried out to allow for their use for energy generation, was reviewed. Finally, for thermal energy generation, the reported work on biopolymer-based devices that work using thermoelectricity has been summarised. In each case, the latest advances in the field from the materials science perspective and the reported performance were described. Hybrid approaches involving the combination of biomass materials with other components have also been considered and compared with the performance obtained using biopolymers alone. Current limitations and opportunities are, finally, discussed to offer an overview of the current landscape and indicate future directions of the field.

Keywords: triboelectric; piezoelectric; cellulose; lignin; osmotic energy; thermoelectric

Citation: Ruiz-Gonzalez, A.; Wang, M.; Haseloff, J. Sustainable Approaches to Incorporate Plant-Based Biomaterials in Power Generation. *Solids* **2023**, *4*, 133–155. https://doi.org/10.3390/solids4020009

Academic Editor: Andrei Kovalevsky

Received: 15 May 2023
Revised: 30 May 2023
Accepted: 30 May 2023
Published: 2 June 2023

1. Introduction

Energy generation from biomass represents a promising alternative to the use of fossil fuels and it will play a pivotal role in achieving the net-zero carbon target by 2050. Biomass refers to the organic material that is obtained from living organisms. The most common route for exploiting the energy contained in biomass is through the combustion of its components. This type of energy is also commonly referred to as "bioenergy". Bioenergy is considered carbon neutral, since its use does not, in principle, lead to the accumulation of net carbon in the atmosphere, since biomass is generated through the fixation of CO_2 by plants. Moreover, the natural decomposition of agricultural or forestry residues releases CO_2, even if they are not used for energy generation [1]. Consequently, this energy source has the potential to reduce the use of underground fossil fuels. Although within the past few years new models and policies have been developed to take into account the

release of greenhouse gases as a consequence of the use of fossil fuels for the production and refinement of biomass, the release of CO_2 by the burning of biomass itself is often disregarded [2]. The use of plant residues for the generation of energy still leads to a significant release of CO_2 to the atmosphere [3], which breaks with the assumption of neutrality from biomass resources [1]. In addition, the increased use of biomass resources for energy production through combustion will inevitably lead to a transformation of natural ecosystems [4]. Thus, alternative routes for energy generation that make use of biomass materials without the need for combustion and that can be reused for long periods of time are needed.

The development of alternative sources of energy, such as solar panels and wind energy, represents a promising alternative to mitigate CO_2 production from fossil fuel consumption, with a high-power yield. However, to allow for a truly renewable energy source, devices must not only involve materials and systems that can harvest energy in an efficient way, but also environmentally friendly materials that do not lead to significant environmental damage during production. The fabrication of some of the components used in renewable energy devices often involves the use of non-sustainable or toxic compounds. An example of these compounds is silicon tetrachloride, which has been shown to have a high environmental impact due to its toxicity [5]. On the contrary, a synthesis of plant-derived biomaterials could theoretically be achieved through "carbon negative" methods, which lead to a storage of CO_2 from the atmosphere given the natural ability of plants to fix carbon. Thus, the incorporation of biomass-derived materials in the fabrication of these renewable energy devices shows a promising approach that could further save environmental and power costs, while overcoming the limitations of biomass combustion.

One of the most common biomass-derived materials is cellulose [6], which is produced at a scale of 1.5 $\times$ 1012 tonnes per year [7]. This material is by far the most studied biomass compound in energy research given its low cost and chemical versatility, and its material shows advantages compared with traditional materials, which enables its incorporation in multiple applications. Cellulose gels show a high porosity and specific surface area, which can enhance energy generation through surface phenomena such as triboelectricity. Moreover, it is a flexible material, with a good ion conductivity when hydrated, which improves the use in portable [8], wearable devices compared with traditional materials. This material can be further modified chemically to enhance power generation through chemical oxidation or click chemistry among others.

Cellulose is an oligosaccharide, formed by D-glucose units, covalently attached by β(14)-bonds. This material is widely available, without the requirement for expensive synthesis or the use of hazardous chemicals. In addition, it can be extracted using low-cost and environmentally friendly methods, either from biomass [9–11] or by bacterial production [12–14]. Unlike most petroleum-based products, cellulose represents a renewable and biodegradable option, with a low environmental impact. Thus, in recent years, the applications of this biopolymer have expanded, and the number of scientific papers and patents being filed in this field have shown a high increase [15].

Within the cell walls of plants, cellulose is present in combination with hemicellulose and lignin (Figure 1a) [16]. Natural lignocellulose is made of a mixture between crystalline and amorphous cellulose fibrils embedded inside a matrix of lignin and hemicellulose. This structure can limit the performance of cellulose in energy harvesting applications given the low electrical conductivity of lignin [17], and it reduces the accessibility of chemical compounds to cellulose fibres such as enzymes, which has an impact on the ability to process cellulose [18]. However, through stripping, cellulose nanofibres can be extracted from natural cellulose, with a diameter in the range of 3–20 nm and a length of 0.5–2 μm [19].

Cellulose is generally insoluble, with good mechanical properties, allowing for its use as a reinforcement material either in the form of nanocomposites [20] or hybrid materials, with the incorporation of other polymers [21]. In addition, it shows a high biocompatibility, enabling its use in biomedical applications such as wearable sensors [22,23] or implantable devices [24,25]. Natural cellulose can be found in the form of microfibres and

presents crystalline domains due to the formation of strong hydrogen bonds between the molecular chains [26]. However, these crystallites represent only a small portion of the material. In its natural state, cellulose crystallites have a size between 25–36 Å in the case of softwoods [27–30]. The crystalline structure of these natural cellulose nanocrystals, the so-called cellulose I, is monoclinic sphenodic (Figure 1b) [31]. Upon swelling or regeneration, this crystal structure can change to cellulose II, with a rearrangement of the hydrogen bonds (Figure 1c) [32].

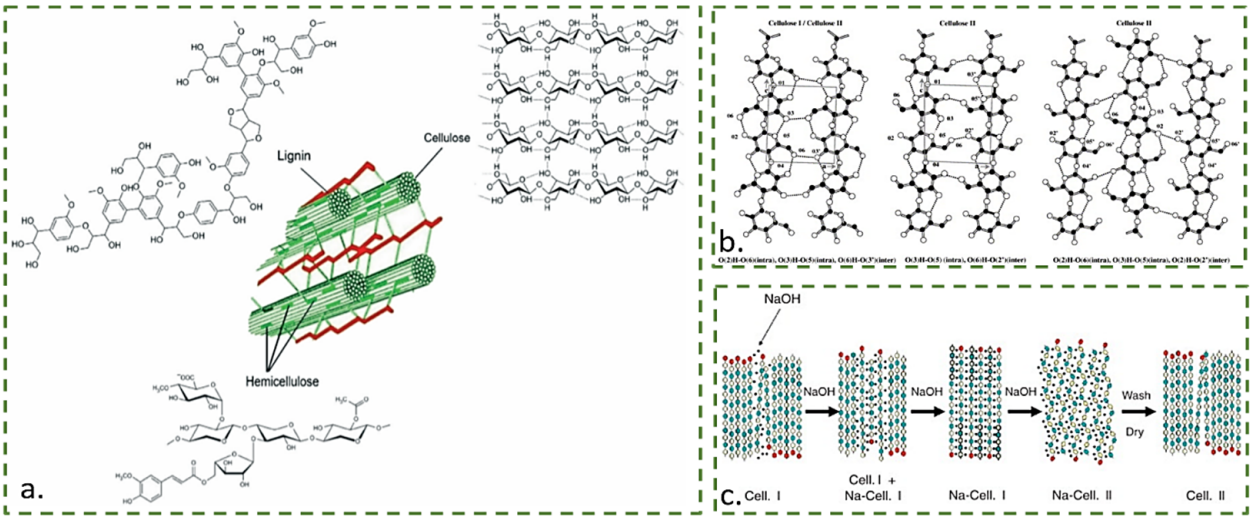

Figure 1. (**a**) Schematic representation of the structure of natural cellulose prior to any chemical treatment, in combination with the two other major components of plant biomass: hemicellulose and lignin. Figure reused with permissions from [33], Copyright RSC (2020). (**b**) Chemical structure of the two major crystalline forms of cellulose: Cellulose I and cellulose II. Figure reused with permissions from [34], Copyright Elsevier Ltd. (2005, Amsterdam). (**c**) Chemical transition between cellulose I to cellulose II upon the use of a strong base (NaOH). Figure reused with permissions from [35], Copyright Elsevier Inc. (2010).

2. Materials and Methods

Natural cellulose can be found as a mixture of its amorphous and crystalline states. To date, six forms of crystalline cellulose have been described, namely cellulose I, II, III_I, III_{II}, IV_I, and IV_{II} [36]. The crystallinity of cellulose and the high presence of hydroxyl groups provides cellulose with a strong electron-donating ability and high number of dipoles, which have been exploited for energy harvesting through tribo- and piezoelectricity [19]. The most common form of natural cellulose is cellulose I. Cellulose II, also called regenerated cellulose, is formed upon modification of the structure of cellulose I using different solvents, including basic solutions containing NaOH [37]. In plants, cellulose is predominantly found as cellulose Iβ, whilst cellulose Iα is obtained from less complex organisms such as bacteria. Both crystalline cellulose structures present a parallel chain arrangement but differ in their lattice systems. Cellulose Iα is a one-chain triclinic system, while Iβ presents a two-chain monoclinic structure [36].

The highly hydroxylated composition of cellulose allows for its easy modification and functionalisation. Surface modification reactions such as oxidation [38,39] or acetylation [40], and surface functionalisation using click chemistry [41], among others, have been carried out in cellulose polymers to improve their chemical properties towards specific applications. These modifications can be performed using green chemistry routes, while preserving its sustainability and biodegradability. As such, there has been a great interest in the incorporation of cellulose and its derivatives into multiple applications such as structural materials [42–44], sensing [45–47], or smart textiles [48,49], among others. In particular, its use in energy harvesting systems has attracted rising interest in the last

few years, given the high versatility of cellulose, which can be easily functionalised and chemically modified to tailor its properties. As such, it represents a renewable and low-cost alternative to current materials employed in energy harvesting.

An alternative material derived from plant biomass is lignin. Lignin is an amorphous macromolecule, which shows a different composition depending on the plant source [50]. In general terms, lignin is formed by three different phenylpropane monomers: *p*-coumaryl alcohol, coniferyl alcohol, and sinapyl alcohol, with variable ratios. However, despite being the second most widespread biopolymer in nature, the applications of lignin in power generation are limited. This fact can be attributed to its poor electrical performance and lower processability compared to cellulose, given the insolubility in inert solvents and chemical stability of lignin [51]. Consequently, the market size for lignin is considerably lower compared to cellulose, being $730 million in 2014 [52], and it is expected to reach $1.6 billion by 2025 [53]. In comparison, the market size for cellulose was 1.72 billion in 2014 and it is expected to reach $7.4 billion by 2025 only within the Asia-Pacific region [54,55], showing a higher volume and growth. However, lignin shows good mechanical resilience and transparency, which could be exploited within biomedical applications such as electronic skins [56] and structural [57] applications.

This review discusses the current landscape of biomass-derived materials, especially cellulose and lignin, in renewable energy generation. Three major areas are discussed: mechanical, osmotic, and thermal energy. Specifically, we focused on approaches where these biomass materials can be used as an active component instead of a mechanical support. In each case, the properties of the biomass materials that are exploited to generate electricity from a fundamental chemical level and how they relate with the observed performance are described. Hybrid materials where multiple chemicals and nanostructured compounds have been combined are also described and their performance is detailed. The review of these materials and their applications allowed for an objective comparison between the performance of different energy sources that could be used to identify potential areas for improvement and opportunities in this field.

3. Energy Generation from Mechanical Movement

3.1. Piezoelectric Generators

Mechanical energy is one of the most ubiquitously available forms of energy in the environment. As such, it represents a large source of renewable power. The piezoelectric effect was first described in quartz crystals by the Curie brothers in 1880. Since then, multiple materials, such as barium titanate, tourmaline, and Rochelle, have been discovered and tested [58]. Piezoelectric generators can produce a change in the electrical polarisation of the active materials as a consequence of an induced mechanical stress. This phenomenon is called the direct piezoelectric effect (Figure 2a). Piezoelectric materials can also deform when they are subjected to an electrical field, defined as the reversed piezoelectric effect (Figure 2b). The piezoelectric effect takes place within materials with no centre of symmetry on their crystal structure. In these materials, a mechanical strain causes an asymmetric shift on the ionic charges in the crystal structure, which generates a voltage. To generate piezoelectricity, the active material must be enclosed between two separate electrodes and, under the application of a mechanical input such as a vibration or pressure, the device generates electricity due to the formation of a voltage difference between the electrodes, allowing for a harvesting of mechanical energy (Figure 2c).

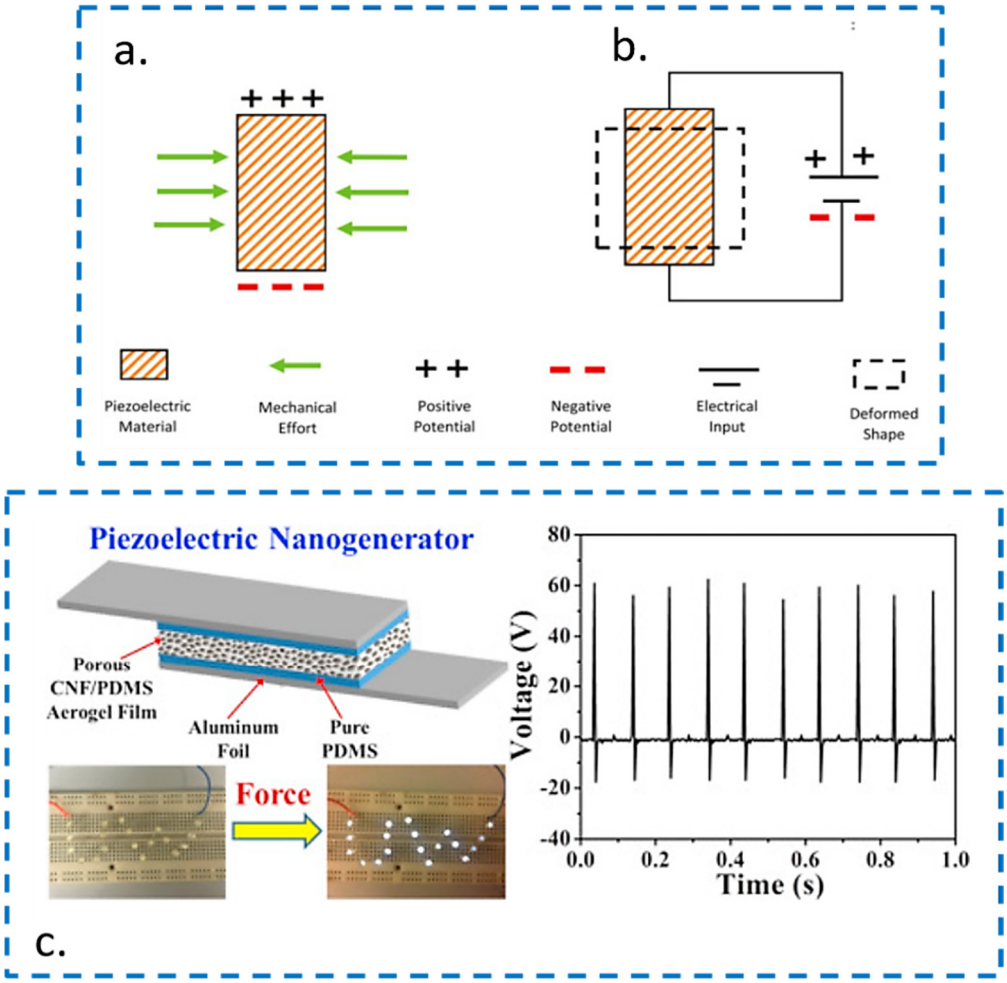

Figure 2. (**a**) Schematic representation of the direct and reverse piezoelectric effect. Piezoelectric generators exploit the direct piezoelectric effect, where a voltage is generated through the application of a mechanical stress. (**b**) Representation of the reverse piezoelectric effect, where a mechanical deformation is driven by an applied voltage. Figures adapted with permissions from [58], Elsevier Ltd. (2021, Amsterdam). (**c**) Example of a piezoelectric nanogenerator, employing cellulose nanofibres for the generation of electricity. Upon the use of a mechanical input, the device could power a group of LEDs due to the generated voltage. Figure adapted from [59], Elsevier Ltd. (2016, Amsterdam).

Cellulose nanocrystals can produce piezoelectricity due to their particular structure, presenting a noncentrosymmetry, with two different hydrogen bonding networks [60,61]. This effect was first reported in 1954 by Fukada [62], who observed the piezoelectric effects on the annual rings of wood. Since then, multiple devices have been designed to exploit this effect using cellulose-based materials. This material has been employed either as a piezoelectric generator or in the form of a nanocomposite, with nanoparticles embedded.

The power yield of the devices based on natural cellulose alone tends to be low compared to commonly used organic materials in piezoelectric generators such as polylactic acid [63] or poly(vinylidene difluoride) (PVDF) [64]. In the case of PVDF, a power output of 112.8 μW has been reported by Song et al. [65], being similar to current ceramic-based harvesters. However, the poor yield of cellulose in comparison is reflected by a low piezoelectric coefficient, which is related to the strength of the piezoelectric effect on the material and indicates the polarisation on the electrodes obtained upon subjecting the material to a mechanical stress. The use of vertically aligned cellulose nanocrystals has been demonstrated to enhance this piezoelectricity generation [66]. The increase in energy generation is a consequence of the large dipole moment of cellulose within the cellulose chain direction [66]. Vertically aligned CNC films

achieved a piezoelectric coefficient of 19.3 ± 2.9 pC/N, which is similar to the one observed in PVDF, in the range of 20–30 pC/N [67]. This piezoelectric coefficient was 50 times higher than the longitudinal piezoelectric coefficient observed in wood cellulose fibres, which has been reported to be 0.4 pC/N [68]. However, the formation of vertically aligned cellulose nanocrystals required the use of a DC voltage of 5 kV, reducing the scalability of the fabrication process industrially.

The piezoelectric coefficient of cellulose can be further increased to up to 210 pm/V when used in the form of ultrathin films of aligned nanocrystals [69]. This value is similar to the one obtained by piezoelectric metal oxides and can be obtained by fabricating the films using a uniform electric field onto a mica substrate. Despite the high piezoelectric coefficient achievable by cellulose nanocrystals, especially by aligned nanocrystals, the expensive fabrication and processing involved make it an impracticable technology within a commercial setup. As such, alternative materials that require a lower degree of chemical processing are desired to reduce the production costs and improve the eco-friendliness of the devices.

Unmodified natural cellulose can be used as a power generator, taking advantage of the naturally occurring nanocrystals in plant tissues. As an example, fresh fruits such as pomelo can be used as the piezoelectric material, with a power yield of 12 $\mu W\ cm^{-2}$ [70], which could represent a promising approach for the generation of energy from biowastes. However, the power conversion of this approach was relatively low when compared to the current commercially available devices. In the case of natural wood, the high presence of lignin and its low elastic compressibility lead to a poor piezoelectric output. To circumnavigate these challenges, Sun et al. [71] tested natural wood that had been partially digested using *G. applanatum*. These fungi could partially remove the lignin and hemicellulose molecules, and altered the structure of cellulose, improving its compressibility (Figure 3a,b). As a consequence, the electrical output of wood increased by 55 times compared to the natural untreated version.

Some attempts have been made to improve the energy generation of cellulose by mixing it with other polymers and organosilicon compounds. Ram et al. [72] developed a piezoelectric generator based on 5 wt% cellulose nanocrystals embedded inside a nylon 11 matrix and using glycerol as a plasticiser to increase the flexibility of the system, which could be easily folded (Figure 3c,d). The final device showed a power output of 500 $\mu W\ cm^{-3}$ when subjected to mechanical impacts. The power yield of polymer-mixed devices could be further improved by the incorporation of polydimethylsiloxane (PDMS) with cellulose nanofibrils. Zheng et al. [59] reported a piezoelectric generator using porous cellulose nanofibrils and coated with PDMS, generating a power density of 6.3 mW/cm^3 (Figure 3e). However, the synthesis of some piezoelectric polymers for the fabrication of these mixed approaches requires the use of precursors from nonrenewable sources, especially in the case of petrochemical polymers [73], and it tends to be energy intensive [74]. Although some efforts have been made within the last few years to improve the sustainable production of certain polymers, including PVDF [75] and nylon 11 [76,77], these approaches are not being used industrially yet.

One of the most common approaches in the development of cellulose-based piezoelectric generators is the use of nanocomposites, where one or more nanomaterials are incorporated. Cellulose nanofibres are typically employed in this area, given their high surface area and good mechanical compressibility (Figure 3f,g). This approach enables a fast and low-cost way to increase the piezoelectric performance of cellulose-based compounds. Materials such as multiwalled carbon nanotubes (CNTs) or $BaTiO_3$ have successfully been used in combination with cellulose to produce high-yield piezoelectric generators. Alam et al. [78] developed a nanocomposite-based piezoelectric generator based on cellulose microfibres and PDMS, incorporating MWCNTbs as the conductive filler (Figure 3h). The final device showed a power density of 9.0 $\mu W/cm^3$, enough to power up 22 LEDs and an LCD screen. In addition, $BaTiO_3$ has been incorporated, generating in the form

of nanocomposites [79], reaching a power density as high as 8.41 μW/cm^3, reported by Choi et al. [79], using nanocellulose and 40 wt% $BaTiO_3$ (Figure 3i,j).

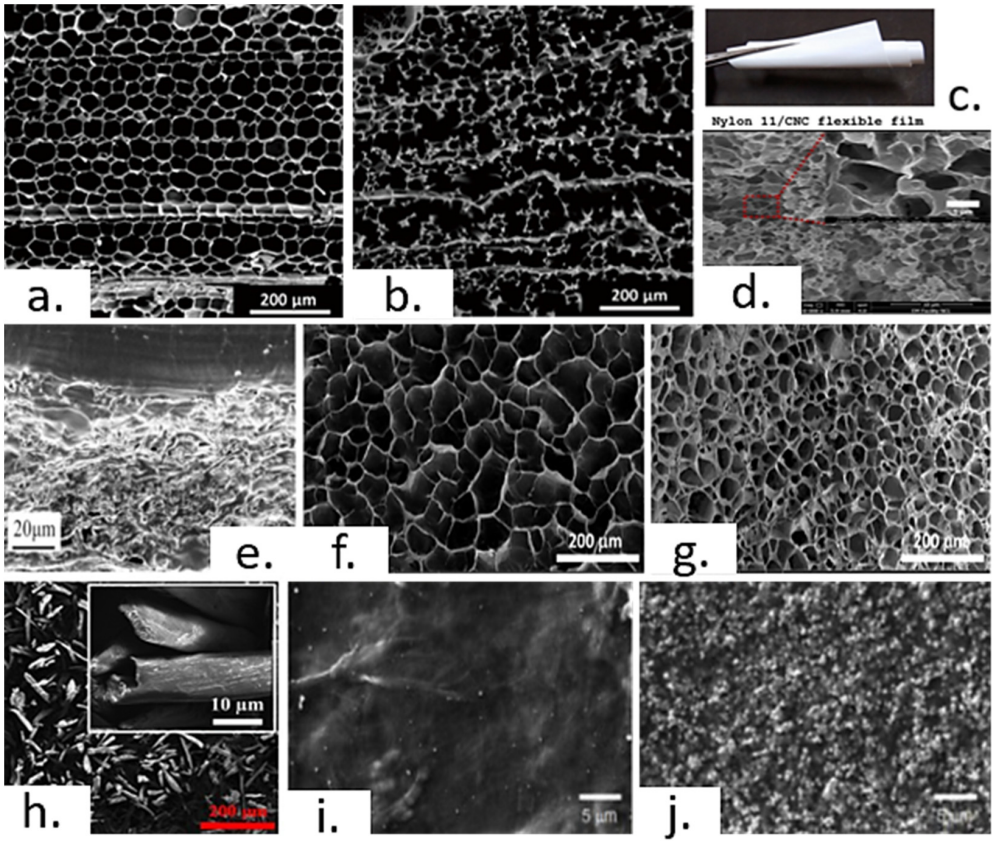

Figure 3. Imaging of different materials employed as piezoelectric generators. (**a**) Structural change in natural cellulose and partially digested cellulose (**b**) obtained using fungi. The chemical and physical changes due to the use of fungi increased the piezoelectric output. Figure adapted from [71] (**c**) Nylon/cellulose nanofibres hybrid device that showed a good flexibility and (**d**) detailed microstructure of the final device. Figures adapted with permissions from [72], Copyright, American Chemical Society (2019). (**e**) Microstructure of a PDMS/cellulose nanofibrils piezoelectric material, reused with permissions from [59], Copyright Elsevier Ltd. (2016). (**f**) Detailed microstructure of cellulose aerogels and (**g**) cellulose aerogel/$BaTiO_3$. Reused with permissions from [80], Copyright Elsevier Ltd. (2018). (**h**) Imaging of crystalline native cellulose. Figure adapted from [78]. (**i**) Surface structure of nanocellulose and (**j**) nanocellulose after the incorporation of barium titanate nanoparticles to enhance the piezoelectric effect. Figures reused with permissions from [79], Copyright Elsevier Ltd. (2019).

The power output of piezoelectric generators can be further increased by combination with triboelectricity, enabling a conversion of mechanical energy into electricity. This concept was applied by Shi et al. [80], who developed a cellulose/$BaTiO_3$ aerogel, increasing the power of the final device from 11.8 μW, when only piezoelectricity was harvested, to up to 85 μW. Thus, the harvesting of mechanical energy through piezoelectricity represents a promising alternative for the powering of devices. However, current piezoelectric generators are limited due to their relatively low power generation and the necessity for a mechanical pressure. As such, new approaches have been developed to enhance this generation of power. A summary of recent approaches in power generation using biomass-derived materials is shown in Table 1.

Table 1. Comparison of the performance of different biomass-derived piezoelectric generators in the literature.

Material	V_{OC}	I_{SC}	Force	Frequency	Power Output	Ref.
PVDF	-	-	-	-	112.8 μW	[65]
Pomelo skin	15 V	130 μA	0.05 N	100 Hz	12 $\mu W/cm^{-3}$	[70]
Wood incubated with *G. applanatum*	0.87 V	13.3 nA	10 N	-	-	[71]
Nylon 11/cellulose nanocrystals	6.95 V	-	23 N	-	500 $\mu W\ cm^{-3}$	[72]
PDMS-coated cellulose nanofibrils	60.2 V	10.1 μA	0.05 MPa	10 Hz	6.3 mW/cm^{-3}	[59]
Cellulose microfibre/PDMS	30 V	500 nA	-	-	9.0 $\mu W/cm^{-3}$	[78]
$BaTiO_3$ -Wood Cellulose fibres	2.86 V	262.35 nA	1 N	1 Hz	8.41 $\mu W/cm^{-3}$	[79]
Cellulose/$BaTiO_3$ aerogel	15.5 V	3.3 μA	80 kPa	3 Hz	11.8 μW	[80]
PVDF-HFP/cellulose nanocrystals	12 V	1.9 $\mu A\ cm^{-2}$	2.5 N	45 Hz	490 $\mu W/cm^{-3}$	[81]
Nitrocellulose nanofibril/ $BaTiO_3$/MWCNT	22 V	220 $nA\ cm^{-2}$	2 $N\ cm^{-2}$	5 Hz	1.21 $\mu W\ cm^{-2}$	[82]
Au nanoparti-cle/cellulose/PDMS	6 V	700 nA	3 N	-	8.34 $mW\ m^{-2}$	[83]
Cellulose/SbSI nanowires	24 mV	-	90 dB	175 Hz	41.5 $nW\ cm^{-3}$	[84]

3.2. Triboelectric Nanogenerators

The concept of triboelectric generators was first reported by Prof. Zhonglin Wang in 2012 [85]. These devices can transform mechanical energy into electricity, even in small amounts of movement. The discovery of this form of energy opened up a new field in renewable energy harvesting and within 12 months of their discovery, the power output of the devices had been improved by 5 orders of magnitude [86].

Power generation through triboelectricity takes place by an electron exchange from an electron-donating material to a charge-trapping layer. As such, this method can combine the energy generated through contact electrification and electrostatic induction and is dependent on the total surface area [87]. When two materials with different surface potentials are put into contact, there is an electron movement that generates an electrical output (Figure 4a) [88]. Common strategies for increasing the power output of triboelectric generators focus on increasing the charges on the active materials or the surface contact between the electrodes. Materials such as modified fluorinated ethylene propylene through ionised gas injection [89] and plasma-treated PDMS [90] have been employed with high output yields. However, these chemical treatments are energy intensive and their scalability for industrial purposes is low.

The incorporation of cellulose as an active material in energy generation through piezoelectricity or triboelectric nanogenerators represents a promising approach to sustainable power generators. As detailed in the previous section, cellulose presents a piezoelectric behaviour due to its crystalline structure. In addition, among all the available biomass-derived compounds, cellulose represents the most widespread material applied to triboelectric generators. Cellulose materials are positively charged in triboelectric terms due to the high amount of oxygen atoms within their molecular structure [91]. This chemical composition allows for the loss of electrons without requiring a high energy. This property of pure cellulose is reflected in a high frictional contact charge transfer, in the range of $-130\ \mu C\ m^{-2}$, being higher than the average value for common polymers [19].

The first cellulose-based triboelectric generator was reported by Yao et al. in 2016. The cellulose was first oxidised with tetramethylpiperidine-1-oxy and paired with fluorinated ethylene propylene as the negative triboelectric layer (Figure 4b,c) [92]. The differences in the polarity between both the treated cellulose and the fluorinated ethylene propylene allowed for its use without the need for any additional material. In addition, an energy harvesting device combining the tribo- and piezoelectric capabilities of cellulose has been reported, with a power output as high as 10.6 $\mu W \cdot cm^{-2}$ for the triboelectric generation and 1.21 $\mu W \cdot cm^{-2}$ for the piezoelectric side [82]. This piezo- and triboelectric hybrid system could also be used as a pressure sensor with a low detection limit of 0.2 N cm^{-2}. This device combined a wood-derived nitrocellulose by modification using nitric acid and a piezoelectric nanocomposite containing $BaTiO_3$/MWCNTbs with bacterial cellulose. However, the power output of power generators can be further improved by focusing on strategies to increase the triboelectric output.

The performance of triboelectric generators is directly proportional to the charge density of the active surfaces and the surface area [93]. As such, one of the main approaches in the development of these devices is the incorporation of different nanoparticles that can enhance the surface area in a cellulose matrix, making a nanocomposite. Materials such as ZnO have been used in the form of biocompatible triboelectric generators, showing a power density of 42 mW m^{-2} (Figure 4d,e) [94]. In addition, $BaTiO_3$ particles have been incorporated into cellulose nanofibres to enhance the surface roughness and dielectric permittivity of the triboelectric generators, increasing the power density by 2 orders of magnitude, with a reported value of 4.8 W m^{-2} [95]. The performance of cellulosic materials can be further increased through the functionalisation of the biopolymer chains with electron-donating groups such as aminated siloxanes [96]. In the case of cellulose aerogels, Zhang et al. [97] reported a method for the synthesis of this material that led to a surface area of 221 m^2 g^{-1} and a maximum power density of 127 mW m^{-2} when used as a triboelectric generator using polytetrafluoroethylene (PTFE) as the back electrode (Figure 4f,g) [95].

Another biomass-derived material that has shown potential for its incorporation into triboelectric generators is lignin. Despite its poor electrical conductivity, the electron-transfer capabilities of lignin could be exploited by placing this material in contact with charge-trapping films such as Kapton [98]. Given the high stiffness and insolubility of lignin, this material had to be combined with starch, and led to a power density of 173.5 nW cm^{-2}. This value resulted in a lower value than the ones observed in cellulose, which explains the scarce amount of approaches exploring lignin as an energy material within the literature.

Although the applications of biomass-derived materials, especially cellulose, are well established within the literature, the overexploitation of this resource could enhance deforestation rates [99]. Consequently, the market for alternative sources for cellulose generation, such as bacterial cellulose, have experienced a high growth within the last few years [100]. However, there is still great interest in the exploitation of whole plants for energy harvesting, which could improve the sustainability of the devices.

As mentioned, power generation through triboelectricity is dependent on the surface area of the employed electrodes [87]. As such, to achieve a good performance, the materials have to be processed through lithography [101] or electrospinning [102]. These methods increase the production costs, limiting their commercialisation. Some plant organs, such as leaves and petals, present a large surface area due to their structure, with a hierarchical porosity and high roughness. In the case of leaves, the presence of cuticle and stoma cells can increase the surface area by up to 170 m^2 g^{-1} for tobacco plants [103]. This surface area value is similar to and even larger than other engineered materials already incorporated as triboelectric generators such as cellulose hydrogels [97,104,105]. As such, plant leaves have been employed as templates for the fabrication of high surface area electrodes for the generation of triboelectricity using PDMS [106]. PDMS elastomer can be used as a negative friction layer in triboelectric generators and it can be patterned using laser ablation to enhance the surface area. Using this method, Lee et al. [107] developed a triboelectric nanogenerator able to produce 7.69 W m^{-2}. Moreover, by using micropatterned PDMS with

incorporated silver nanowires and in contact with human skin, Sun et al. [106] reported a power conversion of 56 V and 3.1 µA (Figure 4h,i). This method could lead to a performance almost 60 times higher than similar devices fabricated using laser ablation [108], saving costs and reducing complexity in the manufacturing.

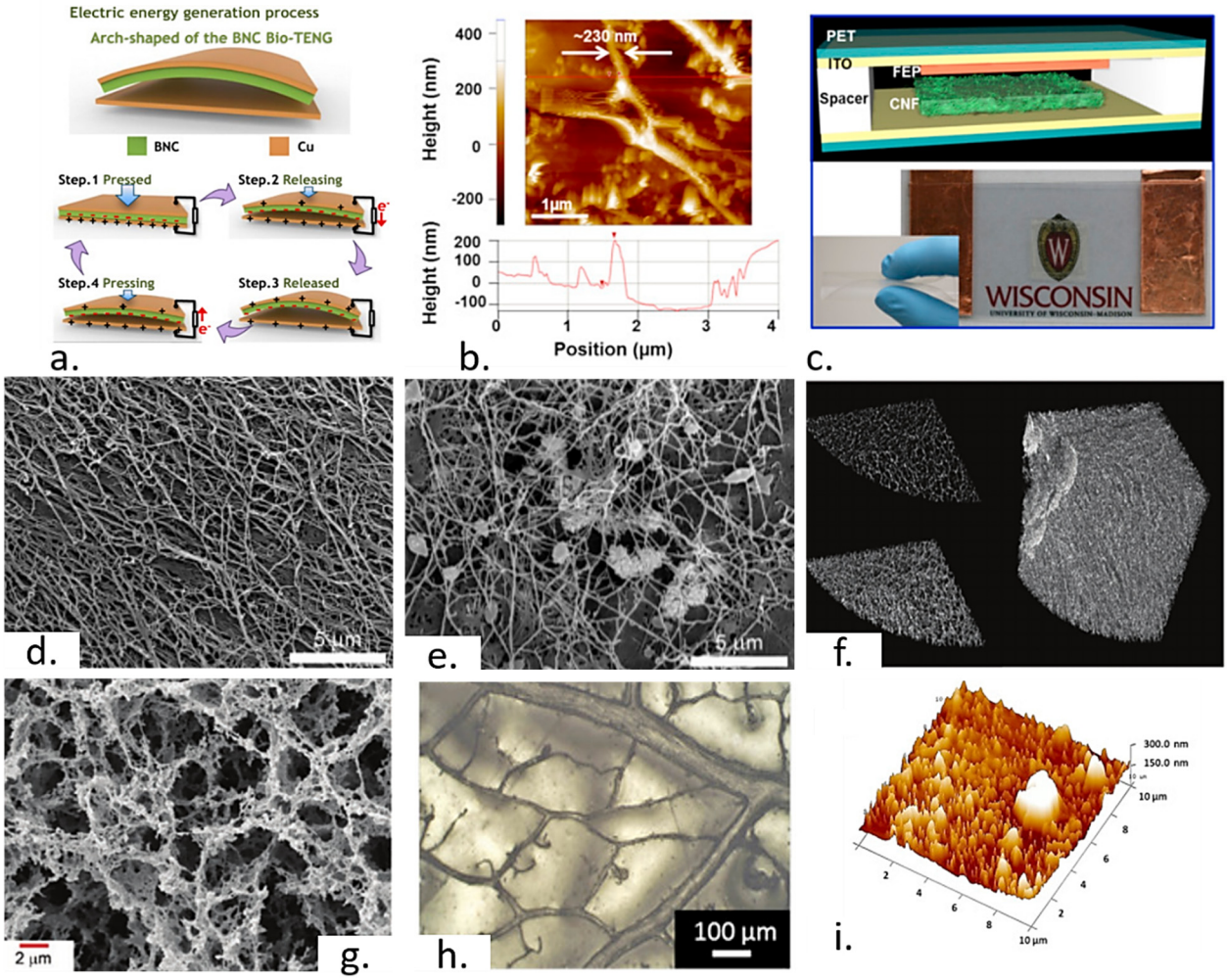

Figure 4. (**a**) Schematic representation of the general structure of triboelectric generators to generate energy from movement. Reused with permissions from [109], Elsevier Ltd. (2017). (**b**) AFM imaging of cellulose nanofibres and the height profile, indicating the average height of the fibres. (**c**) Schematic (top) and real (bottom) representation of the flexible triboelectric generator using cellulose nanofibres and fluorinated ethylene propylene. Figures reused with permissions from [92], Copyright Elsevier Ltd. (2016). (**d**) Morphology of pristine bacterial cellulose and (**e**) bacterial cellulose with incorporated ZnO nanoparticles. Adapted from [94]. (**f**) X-ray nanocomputerised tomography of cellulose aerogels evidencing the fibre network. (**g**) Scanning electron microscopy of cellulose aerogel. Images reused with permissions from [97], Copyright Wiley (2020). (**h**) Morphology of PDMS casted using a plant leaf to increase the surface area and (**i**) AFM profiling of the final device evidencing the increase in surface area. Reused with permissions from [106], Copyright Elsevier Ltd. (2016).

Unmodified plant leaves have a low electron affinity, which can also be exploited to generate a current when it is placed into contact with materials with higher electron affinities such as poly-methyl methacrylate (PMMA). Jie et al. [110] compared the performance of different leaves from multiple tree species and obtained a maximum output power of 45 mW m^{-2} in the case of Hosta leaves. This power output resulted in higher yields than in some of the nanocomposite-based approaches reported. The energy yield of these plants could be greatly improved by the modification of leaf powder with poly-L-lysine

(PLL) [111]. By applying this method, a maximum of 17.9 mW was obtained, which was enough to power a group of 868 LEDs. Thus, the use of whole plants in energy generation has been proven to be a promising alternative for the development of triboelectric generators with a high yield. However, the performance of this approach still cannot meet the high power output of cellulose nanofibres and commercially available devices. A summary of the reported values for cellulose-based triboelectric generators is provided in Table 2.

Table 2. Comparison of the performance of different biomass-derived triboelectric generators in the literature.

Material	V_{OC}	I_{SC}	Force	Frequency	Power Generation	Ref.
Nanopatterned PDMS	414.63 V	40.03 µA	-	-	7.69 W m^{-2}	[107]
Nitrocellulose nanofibril/ $BaTiO_3$/MWCNT	37 V	1.23 µA cm^{-2}	2 N cm^{-2}	5 Hz	10.6 µW cm^{-2}	[82]
Regenerated cellulose	300 V	2.6 mA	-	5 Hz	307 W m^{-2}	[91]
Cellulose nanofibrils	10–30 V	10–90 µA	-	10–60 Hz	-	[92]
Bacterial cellulose/ZnO nanoparticles	57.6 V	5.78 µA	2 N	5 Hz	42 mW m^{-2}	[94]
Bacterial cellulose/$BaTiO_3$ particles	181 V	21 µA	42 N	2 Hz	4.8 W m^{-2}	[95]
Aminosilane-functionalised cellulose nanofibril	195 V	13.4 µA	-	-	-	[96]
Cellulose II aerogel	65 V	1.86 µA	40 N	4 Hz	127 mW m^{-2}	[97]
Lignin/starch	1.04 V cm^{-2}	3.96 nA cm^{-2}	-	0.5 Hz	-	[98]
Micropatterned PDMS	56 V	3.1 µA	-	-	-	[106]
Hosta leaf	230 V	9.5 µA	-	2 Hz	45 mW m^{-2}	[110]
Dry leaf modified with Poly-L-Lysine	1000 V	60 µA	-	5 Hz	-	[111]
Black phosphorous encapsulated with hydrophobic cellulose oleoyl ester nanoparticles	250–880	0.48–1.1 µA	5 N	4 Hz	0.52 mW cm^{-2}	[112]
Lignin/PDMS	308 V	61.6 µA	10 N	30 Hz	5.93 W m^{-2}	[113]

4. Osmotic Energy Harvesting with Cellulose

Whilst the generation of electricity through mechanical energy has been shown to be an efficient way to harvest electrical energy, especially for the powering of wearable devices through human motion, this approach cannot meet the current energetic needs that would enable a reduction in non-renewable energy sources. Thus, alternative renewable forms of energy are required. In recent years, osmotic energy has been developed as an alternative form of power generation. This type of energy is collected from the differences in concentration between two electrolyte solutions. Given the high abundancy of naturally occurring mixtures of fresh and salt water on Earth, especially at the estuaries, it has been estimated that, potentially, up to 2 trillion watts from the environment could be harvested using this technology [114].

The most common method used to generate electrical power through salinity changes is reverse electrodialysis. The first demonstration of this type of energy was reported by Pattle in 1955, using a stack of 94 polyethylene and polystyrene membranes, which generated an external power of 15 mW [115]. Since then, the power output of reverse electrodialysis has greatly improved, with up to 67 W m^{-2} achieved by a single membrane by employing nanoporous and atomically thin carbon-based membranes [116]. Typical electrodialysis systems employ a stack of alternating cation and anion-selective membranes (Figure 5a). As such, the performance of the devices is directly proportional to the properties of the ion-exchange membranes [117]. A highly concentrated salt solution is then used in contact with these ion membranes, separated from a low-concentrated water solution in contact with the membranes as well. The differences in potential between the low-concentrated solutions due to the diffusion of cations and anions, which is driven by the electrochemical gradient with the salt-concentrated solution, generate a voltage [118]. A first pilot plant ex-

ploiting this technology has already been implemented in the Netherlands by the REDStack company, being able to generate several watts per square metre of membrane [119].

Recent discoveries in the field of ion-exchange membranes have allowed for the development of high-performance reverse osmotic systems. However, the further improvement in reverse electrodialysis technologies relies on the discovery of affordable and sustainable materials that can be employed for energy generation. One of the main limitations of this technology, that hinders its full incorporation at an industrial scale, has been the relatively low power efficiency compared to other renewable energy sources. This power efficiency is directly related to the selectivity [114], the charge density, and the conductivity [120] of the ionic-exchange membranes. To improve the power conversion of current osmotic systems, nanoporous materials, such as MXenes [121], boron nitride [122], or graphene [123], have been employed. The porosity and permeation paths of these nanomaterials are located at the sub-nanometre range, allowing for a good selectivity on the cations [124]. However, the diffusion speed of water molecules and ions within such confined compartments is reduced, compromising the performance of the system [119]. In addition, the manufacturing costs of these materials is high, reducing the possibility of scale up.

The incorporation of cellulose-based materials has been proven to be a promising alternative for the fabrication of porous membranes for osmotic energy generation. Specifically, the use of cellulose nanofibrils has demonstrated a high yield performance compared to traditional systems due to its high porosity [125] and the presence of highly polar hydroxyl groups at the surface of cellulose. These properties provide cellulose with a high ion conductivity, which can be further enhanced through chemical functionalisation, such as oxidation [126]. Consequently, cellulose has been employed as a sustainable alternative for ion-exchange membranes in fuel cell applications, among others [127].

Cellulose can be used either in its pure form, after chemical modification [128], or in the form of hybrid materials, with the incorporation of other nanostructured compounds. In the case of hybrid materials, the combination of graphene oxide nanoplatelets and cellulose nanofibrils in the form of assembled layers has been shown to improve the performance of current osmotic energy systems by enlarging the nanochannels while showing a large space charge [124]. These properties can decrease the transfer energy of cations and maintain a good selectivity. Wu et al. [124] implemented this principle for the elaboration of a RED system that could generate up to 4.19 mW m^{-2} using a graphene oxide nanocomposite, generating a layered structure (Figure 5b). However, although in recent years, the feasible synthesis of graphene oxide using environmentally friendly methods has been reported [129–131], the main approach used commercially due to cost-effectiveness is based on modified Hummers methods [132–134]. These methods involve an exfoliation step, where strong oxidants and concentrated sulphuric acid are used. Thus, to achieve a true renewable and environmentally free generation of electricity using this technology, green materials are needed. Cellulose can also be used as a modifier for standard ion-exchange membranes, increasing the charge density of the films [135]. In this case, cellulose acetate was used as a modifier of the standard PVC-based cation membrane. The incorporation of this cellulose modification could reduce the electrical resistance of the films, from 6.77 up to 3.10 Ω cm^2 whilst increasing the charge density by 3 mEq g^{-1}. However, the efficiency of this modification has not been tested yet within a practical device.

The use of cellulose-based nanoporous materials alone has been explored by Wu et al. [136], who reported an efficiency of 0.23 W m^{-2}. To achieve this efficiency, the cellulose nanofibrils had to be functionalised to acquire the negative and positive charges needed for the separation of cations and anions, respectively (Figure 5c,d). In the case of positively charged films, the membranes were modified with quaternary amine groups using etherification. On the contrary, to charge the membranes negatively, carboxyl groups were introduced through 2,2,6,6-tetramethylpiperidine-1-oxyl (TEMPO) oxidation. This approach led to an output power density of 0.23 W m^{-2}, showing promise for an industrially scalable and low-cost device.

One alternative to replace the nanoporous materials is to take advantage of the naturally occurring porosity in wood and cellulose nanofibres. Wu et al. [117] employed a similar strategy to negatively and positively charge wood sheets using TEMPO and etherification, respectively (Figure 5e,f). However, in this case, the power output of the system was considerably lower than the one reported using cellulose nanofibrils alone, with 5.14 mW m^{-2} [117].

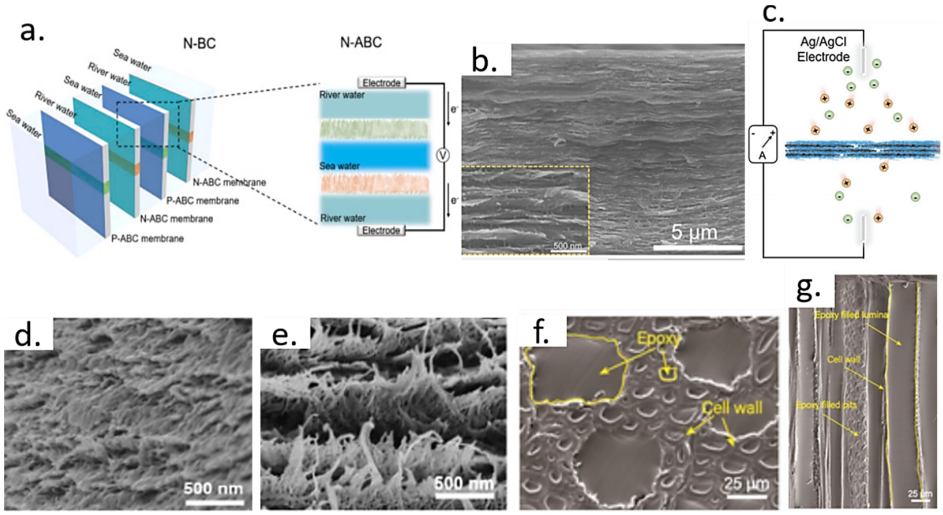

Figure 5. (**a**) Schematic representation of the reverse dialysis process, employing a stack of ion-exchange membranes and a water source that generates a concentration gradient. Reused with permissions from [136], Copyright Elsevier Ltd. (2020). (**b**) Morphology of Graphene oxide/cellulose nanofibres used within a reverse dialysis system. (**c**) Schematic representation of the final device, employed for energy generation. Figures reused with permissions from [124], Copyright Royal Society of Chemistry (2020). (**d**) Cross-sectional imaging of negatively charged cellulose obtained by oxidation. (**e**) Cross-sectional imaging of a positively charged bacterial cellulose obtained by quaternisation. Figures reused with permissions from [136], Copyright Elsevier Ltd. (2020). (**f**) Scanning electron microscopy imaging of the porous surface in negatively charged wood. (**g**) Cross-sectional analysis of the negatively charged wood incorporating an epoxy resin. Figures reused with permissions from [117], Copyright Wiley (2019).

Despite the low power output achieved in the case of lignin-based devices, which could be a consequence of the presence of less ionically conductive materials within wood such as lignin and hemicellulose, the price of each ion-exchange membrane was in the range of $10, which is considerably lower than the commercially available ones (about $350). However, the performance was significantly lower than the one obtained by the cellulose-based approaches. The reported values for lignin- and cellulose-based osmotic energy generators are shown on Table 3.

Table 3. Table summary of reported results using osmotic energy generators.

Material	Power Output	Charge Density (Cation Film)	Charge Density (Anion Film)	Ionic Conductivity (Cation Film)	Ionic Conductivity (Anion Film)	Ref.
Polyethylene/polystyrene	15 mW	-	-	-	-	[115]
Polycyclic aromatic hydrocarbon	67 W m^{-2}	-	-	-	-	[116]
Nanocellulose	0.23 W m^{-2}	3.13 mC m^{-2}	−2.66 mC m^{-2}	0.42 mS cm^{-1}	1.0 mS cm^{-1}	[136]
Cellulose nanofibrils/graphene oxide	4.19 W m^{-2}	-	-	-	-	[124]
Ionised wood	5.14 mW m^{-2}	2.25 mC m^{-2}	−3.09 mC m^{-2}	0.4 mS cm^{-1}	0.2 mS cm^{-1}	[117]
Cellulose oxide/graphene oxide	0.53 W m^{-2}	-	−3.00 mC m^{-2}	-	0.8 mS cm^{-1}	[137]

5. Thermoelectric Energy Harvesting with Cellulose

Thermoelectricity can make use of temperature gradients to generate an electric voltage. This technology is based on the Seebeck effect and has been proven to be a useful tool in the development of self-powered electronics, which can work with the residual heat from the human body [138,139]. In addition, thermoelectricity can be employed to recover energy from waste heat sources such as internal combustion engines [140] or electrical ovens [141], among others.

The energy conversion of thermoelectric materials is indicated by the Seebeck coefficient, which is defined as the ratio between the electromotive force and the temperature difference. However, the performance of thermoelectric materials is commonly described in terms of the "Figure of merit", which includes the contributions from the electrical conductivity of the device, the thermal conductivity, and the Seebeck coefficient (Equation (1)), and it is related to the energy conversion efficiency of the device.

$$zT = \frac{\sigma S^2 T}{k} \quad (1)$$

where σ represents the electrical conductivity, S is the Seebeck coefficient, k is the thermal conductivity, and T is the temperature. From this equation, it can be deduced that materials with a high electrical conductivity and Seebeck coefficient, and low thermal conductivity, are desired. However, since these variables are strongly correlated, a single improvement in one of these is usually compensated for by the rest of the parameters, making it difficult to enhance the value of zT [142]. One of the most common elements found in thermoelectric devices is tellurium. The most widely employed materials in conventional devices are telluride-based semiconductor materials such as Bi_2Te_3 and PdTe. Recently, Bi_2Te_3 thin films were used to develop flexible thermoelectric devices, achieving a power density of 2.1 mW cm^{-2} and a power factor as high as ~200 μW m^{-1} K^{-2} [143]. These materials present a zT of about 1 and are commonly used commercially given their good thermoelectric properties. As such, it can be incorporated inside bacterial cellulose nanofibres, showing a high Seebeck coefficient, in the range of 135 μV K^{-1}, and a power conversion of 25.5 μW m^{-1} K^{-2} [144]. In addition, cellulose nanofibre/Bi_2Te_3 nanocomposites have been applied to wearable devices, increasing the performance by doping the Bi_2Te_3 with selenium and antimony [145]. However, Te is a relatively scarce element, which has propelled research into Te-free devices [146]. In addition, the synthesis of current thermoelectric materials, especially Bi_2Te_3, is carried out by a hydrothermal reaction [147–149], where the precursors need to be subjected to high temperatures and pressure, and requires toxic-reducing agents such as $NaBH_4$ and N_2H_4. Thus, the development of alternative materials with thermoelectric properties that can be synthetised using green and eco-friendly processes represents a crucial aspect in the research of thermoelectric materials.

Plant-derived biomass materials such as cellulose or lignin do not show any thermoelectric properties under standard conditions. However, cellulose chains can be oxidised to improve ionic conductivity and ions can be infiltrated [150]. This approach can generate a voltage due to the movement of ions inside the cellulose fibres when they are subjected to a temperature gradient. Li et al. [150] demonstrated this concept using natural cellulose that had been treated to remove hemicellulose and lignin, making cellulose II membranes. This cellulose was oxidised using 2,2,6,6-tetramethylpiperidine-1-oxyl to increase the negative charge density of the fibres, and Na^+ ions were infiltrated using NaOH. This device showed a thermal gradient ratio of 24 mV K^{-1} and a power factor of 1150 μW m^{-1} K^{-2}. However, the most common approach in the development of cellulose-based thermoelectric materials is their use as a matrix for the fabrication of nanocomposites.

One of the most common materials to provide thermoelectricity to cellulose-based nanocomposites are CNTs. This material has been reported to have a high Seebeck coefficient, which is dependent on its structure. Up to 160 μV K^{-1} at room temperature have been measured for single-walled CNTs and 80 μV K^{-1} in the case of multiwalled CNTs [151]. Thus, it shows promise for the development of highly efficient and flexible devices. CNTs can be

incorporated into cellulose aerogels, either in the form of single- or multiwalled CNTs. As expected, both the Seebeck coefficient and power factor resulted in higher yields in the case of the single-walled CNTs, with 1.1 μW m^{-1} K^{-2} and 47.2 μV K^{-1}, respectively (Figure 6a) [152]. The fabrication process of cellulose-based thermoelectric generators was further simplified by Abol-Fotouh et al. [153], who used a solution containing 0–12 wt% of single-walled CNTs in direct contact with cellulose-making bacteria (K. xylinus), leading to a higher power factor compared to the previous approach, with 20 μW m^{-1} K^{-2}, and a similar Seebeck coefficient (30 μV K^{-1}). However, the morphology obtained through this approach did not show any CNT bundle which led to a difference in the performance (Figure 6b,c). The properties of these nanocomposites can also be tailored by using heteroatom-doped CNTs [154]. Such doping can lead to negative Seebeck coefficients in the range of −20 μV K^{-1} when nitrogen was used as a dopant and positive coefficients (~25 μV K^{-1}) when boron was used. Additional plant biomass-derived materials such as lignin can also be used in this field. Culebras et al. [155] developed CNT yarns doped with lignin produced from lignocellulosic waste. The use of lignin increased the Seebeck coefficient from ~50 μV K^{-1} up to 98.9 μV K^{-1} and the power factor from ~20 μW m^{-1} K^{-2} up to 132.2 μW m^{-1} K^{-2}. Flexible thermoelectric generators have additionally been designed by using natural cellulose, extracted from flax, and combining it with graphene and Bi_2Te_3. The final material presented a layered structure that maximised the contact area (Figure 6d). However, the power factor of this material was relatively low when compared to the cellulose–graphene and cellulose–Bi_2Te_3 nanocomposites alone, showing a power factor of 6.4 × 10^{-2} μW m K^{-2} and a Seebeck coefficient in the range of 20–30 μV K^{-1} at 52 °C [156].

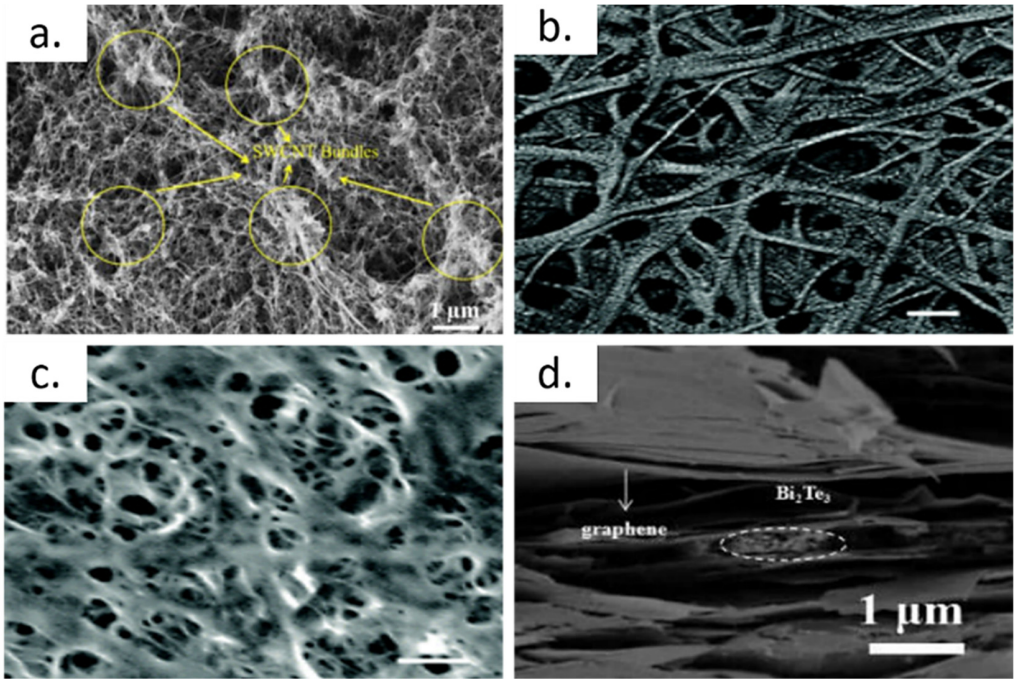

Figure 6. (**a**) Scanning electron microscopy image of a thermoelectric device containing cellulose nanofibres and multi-walled CNTs. The presence of CNT clusters is highlighted. Reused with permissions from [152], Copyright Elsevier Ltd. (2018). Imaging of pristine bacteria cellulose (**b**) and bacteria cellulose after the incorporation of single-walled carbon nanotubes (**c**) Figures adapted from [153]. (**d**) Layered structure of a Bi_2Te_3/graphene/lignin hybrid material, where the lignin has been obtained from lignocellulosic waste. Figure adapted from [155].

Thus, the use of biopolymer-based materials represents an emerging material in the field of thermoelectric generators. The performance of the different reported thermoelectric materials based on biomass-derived materials is detailed on Table 4.

Table 4. Summary of different materials and the thermoelectric performance reported in the literature.

Materials	Power Factor ($\mu W\ m^{-1}\ K^{-2}$)	Seebeck Coefficient ($\mu V\ K^{-1}$)	Figure of Merit	Ref.
Ag-doped Bi_2Te_3	200	-	1.2	[143]
Cellulose ionic conductor	1150	24	-	[150]
Bi_2Te_3/bacterial cellulose	25.5	135	-	[144]
CNF/$Bi_{0.5}Sb_{1.5}Te_3$	-	154	-	[145]
CNF/$Bi_2Se_{0.3}Te_{2.7}$	-	−130	-	[145]
CNT/bacteria cellulose	20	30	2×10^{-3}	[153]
Boron-doped CNTs/ethyl cellulose	-	~25	$\sim 8 \times 10^{-6}$	[154]
Nitrogen-doped CNTs/ethyl cellulose	-	~−20	$\sim 3 \times 10^{-5}$	[154]
Lignin-doped carbon nanotube yarns	132.2	100	-	[155]
Graphene nanoplatelets/ethyl cellulose	0.254	15–20	-	[157]

6. Current Limitations and Opportunities

As observed, despite the high performance of cellulose nanofibres within most of the energy generation applications, they need to be extracted from natural sources. As such, one of the main limitations of biomass-derived materials is the need for processing prior to their use. This is a consequence of the presence of undesired materials on the natural sources such as lignin and hemicellulose and, in some cases, the higher surface area obtained when using cellulose nanofibres. Thus, within all the reported approaches, the utilisation of pure cellulose outperforms unmodified lignocellulose. An opportunity in this field would be the development of simpler and more sustainable chemical routes to purify cellulose from its natural source and chemically modify it with desired functional groups. In addition, the genetic modification of existing plant resources to produce varieties that produce less lignin/hemicellulose could represent an alternative to increase the power output whilst further reducing the fabrication costs.

Despite all the current efforts to use biomass-derived materials as substituents for traditional compounds in power generation, their performance is still considerably lower than some of the recently reported devices. This fact is more prominent within thermoelectric systems, given the low number of reported approaches employing cellulose or lignin. Consequently, the use of hybrid approaches involving cellulose and different nanomaterials still shows the highest performance compared to cellulose alone. As such, another potential opportunity in the improvement in energy generation using biomass-derived materials would be the synthesis of more sustainable fillings that could be used to improve the performance of cellulose. This includes the development of chemical routes to efficiently transform biomass materials into high-performance nanomaterials such as carbon nanotubes and graphene.

Future developments in the field of power generation using biomass-derived materials will focus on the development of high throughput cellulose sources that require minimal processing to achieve a good performance. An example of a potential source is bacterial cellulose which, as observed, presents good physical–chemical properties given the high presence of nanofibrils that enhance the surface area of materials. However, this method for cellulose generation is slow and requires a high energy to maintain bacterial colonies.

In addition to the chemical modification of cellulose biopolymers, the advantage of using vertically aligned nanocrystals has been described. This material can be used to achieve a high piezoelectric coefficient, leading to an enhanced power generation. Further developments in the manufacturing of thin nanocrystalline cellulose films could be incorporated into miniaturised and wearable sensors that will make use of the power generation

for battery-less health monitoring. In this context, cellulose films could be used both as a power source for low-power electronics and as sensing materials. The piezoelectric and triboelectric properties of cellulose could be exploited to determine hand movement or muscle contractions, among other applications, while thermoelectric generators could be used as temperature sensors. Moreover, the mechanical versatility of cellulose thermoelectrics could be used in the harvesting of waste heat directly from the generating source. This could enable the recovery of power from small electronic parts, such as electric wires, directly, boosting the efficiency.

Finally, the unprecedented development in materials science and engineering in the last few years will eventually allow for the design of more efficient energy harvesting devices, which would take full advantage of the properties of biomass-derived compounds.

7. Conclusions and Remarks

In summary, this review describes the latest developments in the use of biomass-derived polymers, such as cellulose or lignin, to be applied to the generation of renewable energies. These materials have not only been chosen due to their low cost and sustainability, but also due to their good performance when employed in energy generation.

In the case of cellulose, the complex chemical structure, comprising both amorphous and crystalline domains, allows for the tailoring of its chemical properties to enhance the power yield. Its chemical structure can also be modified to improve its conductivity or charge density. In particular, the crystalline domains in cellulose can generate piezoelectricity due to its noncentrosymmetry, which has been exploited to develop energy harvesting devices. However, so far, the highest yield in these devices based on biomass materials has been reported in the case of nanocomposite materials. Despite the enhanced output achieved by nanocomposite-based piezoelectric generators, there is great interest in the use of biomass materials from low-cost sources to improve the possibility of scale up and manufacturability within a commercial setup. This form of power generation, using cellulose only, is higher when aligned cellulose nanocrystals are employed. However, an electrical output can also be obtained from natural cellulose obtained from certain plant structures, such as pomelo fruit or wood, greatly reducing the time and energy required for the fabrication of power generators.

The development of triboelectric generators has expanded the possibilities for the utilisation of biomass materials in energy harvesting. Cellulose presents a relatively high charge density due to the presence of hydroxyl groups within its surface. In addition, this material shows a high surface area when used in the form of nanofibres. As such, in general terms, the reported power generation rates in the case of triboelectric-based devices employing cellulose tend to be higher than piezoelectric generators. However, the versatility of cellulose molecules has allowed for the design of hybrid devices able to harvest energy employing piezoelectricity and triboelectricity sources.

Another potential field where the use of biomass-derived materials could be incorporated is osmotic energy generation. This method represents a more optimal route to obtain energy from the environment, since the mixture between water sources containing different salinities occurs naturally at estuaries. The possibility of chemically modifying cellulose plays a pivotal role in this technology, since positively and negatively charged membranes can be synthetised through quaternisation and oxidation, respectively. Both natural lignocellulose and cellulose nanofibres have been incorporated in this field. However, the highest yield was achieved by using graphene oxide-based nanocomposites. Among the studied methods in this manuscript, osmotic energy represents the most promising approach to replace traditional carbon-based energy generators, given the high-power output, and the possibility of scaling up the size of the generators.

Contrary to the approaches previously mentioned, the use of biomass materials in thermoelectricity has not been extensively studied and the number of described approaches in the literature is scarce. The use of pure cellulose as an active material by the oxidation of cellulose nanofibres and infiltration of ions has been demonstrated, with a high-power

factor and Seebeck coefficient. However, the most popular approach involves the incorporation of carbon nanotubes to form complex nanocomposites. Thus, there is a need for the development of simple and low-cost high-yield thermoelectric generators based on biomass materials exclusively.

Funding: This research was funded by the Soil programme, from NERC-NSF, phytoelectric soil Sensing (NE/T012293).

Conflicts of Interest: The authors declare no conflict of interest.

References

1. Booth, M.S. Not carbon neutral: Assessing the net emissions impact of residues burned for bioenergy. *Environ. Res. Lett.* **2018**, *13*, 035001. [CrossRef]
2. Bird, D.N.; Pena, N.; Frieden, D.; Zanchi, G. Zero, one, or in between: Evaluation of alternative national and entity-level accounting for bioenergy. *GCB Bioenergy* **2012**, *4*, 576–587. [CrossRef]
3. Haberl, H.; Sprinz, D.; Bonazountas, M.; Cocco, P.; Desaubies, Y.; Henze, M.; Hertel, O.; Johnson, R.K.; Kastrup, U.; Laconte, P.; et al. Correcting a fundamental error in greenhouse gas accounting related to bioenergy. *Energy Policy* **2012**, *45*, 18–23. [CrossRef] [PubMed]
4. Haberl, H.; Erb, K.H.; Krausmann, F.; Gaube, V.; Bondeau, A.; Plutzar, C.; Gingrich, S.; Lucht, W.; Fischer-Kowalski, M. Quantifying and mapping the human appropriation of net primary production in earth's terrestrial ecosystems. *Proc. Natl. Acad. Sci. USA* **2007**, *104*, 12942–12947. [CrossRef] [PubMed]
5. Yang, H.; Huang, X.; Thompson, J.R. Tackle pollution from solar panels. *Nature* **2014**, *509*, 563. [CrossRef]
6. Lourdes Ballinas-Casarrubias, A.C.-D.; Gutierrez-Méndez, N.; Ramos-Sánchez, V.H.; Flores, D.C.; Manjarrez-Nevárez, L.; Zaragoza-Galán, G.; González-Sanchez, G. Biopolymers from Waste Biomass—Extraction, Modification and Ulterior Uses. In *Recent Advances in Biopolymers*; Perveen, F.K., Ed.; IntechOpen: London, UK, 2015.
7. Klemm, D.; Heublein, B.; Fink, H.-P.; Bohn, A. Cellulose: Fascinating Biopolymer and Sustainable Raw Material. *Angew. Chem. Int. Ed.* **2005**, *44*, 3358–3393. [CrossRef]
8. Dandegaonkar, G.; Ahmed, A.; Sun, L.; Adak, B.; Mukhopadhyay, S. Cellulose based flexible and wearable sensors for health monitoring. *Mater. Adv.* **2022**, *3*, 3766–3783. [CrossRef]
9. Yang, J.; Lu, X.; Liu, X.; Xu, J.; Zhou, Q.; Zhang, S. Rapid and productive extraction of high purity cellulose material via selective depolymerization of the lignin-carbohydrate complex at mild conditions. *Green Chem.* **2017**, *19*, 2234–2243. [CrossRef]
10. Abdul Sisak, M.A.; Daik, R.; Ramli, S. Characterization of cellulose extracted from oil palm empty fruit bunch. In *AIP Conference Proceedings*; AIP Publishing LLC: Melville, NY, USA, 2015; Volume 1678, p. 050016.
11. Nazir, M.S.; Wahjoedi, B.A.; Yussof, A.W.; Abdullah, M.A. Green extraction and characterization of cellulose fibers from Oil Palm Empty Fruit Bunch. In Proceedings of the 2nd International Conference on Process Engineering and Advance Material (ICPEAM), A Conference of ESTCON, Kuala Lump, Malaysia, 12 June 2012.
12. Vazquez, A.; Foresti, M.L.; Cerrutti, P.; Galvagno, M. Bacterial Cellulose from Simple and Low Cost Production Media by Gluconacetobacter xylinus. *J. Polym. Environ.* **2013**, *21*, 545–554. [CrossRef]
13. Revin, V.; Liyaskina, E.; Nazarkina, M.; Bogatyreva, A.; Shchankin, M. Cost-effective production of bacterial cellulose using acidic food industry by-products. *Braz. J. Microbiol.* **2018**, *49*, 151–159. [CrossRef]
14. Abol-Fotouh, D.; Hassan, M.A.; Shokry, H.; Roig, A.; Azab, M.S.; Kashyout, A.E.H.B. Bacterial nanocellulose from agro-industrial wastes: Low-cost and enhanced production by Komagataeibacter saccharivorans MD1. *Sci. Rep.* **2020**, *10*, 3491. [CrossRef] [PubMed]
15. Sharma, A.; Thakur, M.; Bhattacharya, M.; Mandal, T.; Goswami, S. Commercial application of cellulose nano-composites—A review. *Biotechnol. Rep.* **2019**, *21*, e00316. [CrossRef] [PubMed]
16. Zeng, Y.; Himmel, M.E.; Ding, S.-Y. Visualizing chemical functionality in plant cell walls. *Biotechnol. Biofuels* **2017**, *10*, 263. [CrossRef] [PubMed]
17. Chupka, É.I.; Rykova, T.M. Electrical properties of lignin. *Chem. Nat. Compd.* **1983**, *19*, 78–80. [CrossRef]
18. Østby, H.; Hansen, L.D.; Horn, S.J.; Eijsink, V.G.; Várnai, A. Enzymatic processing of lignocellulosic biomass: Principles, recent advances and perspectives. *J. Ind. Microbiol. Biotechnol.* **2020**, *47*, 623–657. [CrossRef]
19. Song, Y.; Shi, Z.; Hu, G.-H.; Xiong, C.; Isogai, A.; Yang, Q. Recent advances in cellulose-based piezoelectric and triboelectric nanogenerators for energy harvesting: A review. *J. Mater. Chem. A* **2021**, *9*, 1910–1937. [CrossRef]
20. Dufresne, A.; Belgacem, M.N. Cellulose-reinforced composites: From micro-to nanoscale. *Polímeros* **2013**, *23*, 277–286. [CrossRef]
21. Jawaid, M.; Abdul Khalil, H.P.S. Cellulosic/synthetic fibre reinforced polymer hybrid composites: A review. *Carbohydr. Polym.* **2011**, *86*, 1–18. [CrossRef]
22. Silva, R.R.; Raymundo-Pereira, P.A.; Campos, A.M.; Wilson, D.; Otoni, C.G.; Barud, H.S.; Costa, C.A.R.; Domeneguetti, R.R.; Balogh, D.T.; Ribeiro, S.J.L.; et al. Microbial nanocellulose adherent to human skin used in electrochemical sensors to detect metal ions and biomarkers in sweat. *Talanta* **2020**, *218*, 121153. [CrossRef]

23. Brakat, A.; Zhu, H. Nanocellulose-Graphene Hybrids: Advanced Functional Materials as Multifunctional Sensing Platform. *Nano-Micro Lett.* **2021**, *13*, 94. [CrossRef]
24. Robotti, F.; Sterner, I.; Bottan, S.; Rodríguez, J.M.M.; Pellegrini, G.; Schmidt, T.; Falk, V.; Poulikakos, D.; Ferrari, A.; Starck, C. Microengineered biosynthesized cellulose as anti-fibrotic in vivo protection for cardiac implantable electronic devices. *Biomaterials* **2020**, *229*, 119583. [CrossRef] [PubMed]
25. Petersen, N.; Gatenholm, P. Bacterial cellulose-based materials and medical devices: Current state and perspectives. *Appl. Microbiol. Biotechnol.* **2011**, *91*, 1277–1286. [CrossRef] [PubMed]
26. Chami Khazraji, A.; Robert, S. Interaction Effects between Cellulose and Water in Nanocrystalline and Amorphous Regions: A Novel Approach Using Molecular Modeling. *J. Nanomater.* **2013**, *2013*, 409676. [CrossRef]
27. Bergander, A.; Brändström, J.; Daniel, G.; Sahnen, L. Fibril angle variability in earlywood of Norway spruce using soft rot cavities and polarization confocal microscopy. *J. Wood Sci.* **2002**, *48*, 255–263. [CrossRef]
28. Tanaka, F.; Koshijima, T.; Okamura, K. Characterization of cellulose in compression and opposite woods of a Pinus densiflora tree grown under the influence of strong wind. *Wood Sci. Technol.* **1981**, *15*, 265–273. [CrossRef]
29. Jakob, H.F.; Fengel, D.; Tschegg, S.E.; Fratzl, P. The Elementary Cellulose Fibril in *Picea abies*: Comparison of Transmission Electron Microscopy, Small-Angle X-ray Scattering, and Wide-Angle X-ray Scattering Results. *Macromolecules* **1995**, *28*, 8782–8787. [CrossRef]
30. Andersson, S.; Serimaa, R.; Paakkari, T.; Saranpää, P.; Pesonen, E. Crystallinity of wood and the size of cellulose crystallites in Norway spruce (*Picea abies*). *J. Wood Sci.* **2003**, *49*, 531–537. [CrossRef]
31. Meyers, M.A.; Chen, P.-Y.; Lin, A.Y.-M.; Seki, Y. Biological materials: Structure and mechanical properties. *Prog. Mater. Sci.* **2008**, *53*, 1–206. [CrossRef]
32. Rosenau, T.; Potthast, A.; Hofinger, A.; Bacher, M.; Yoneda, Y.; Mereiter, K.; Nakatsubo, F.; Jäger, C.; French, A.D.; Kajiwara, K. *Toward a Better Understanding of Cellulose Swelling, Dissolution, and Regeneration on the Molecular Level, In Cellulose Science and Technology*; John Wiley & Sons, Inc.: Hoboken, NJ, USA, 2018; pp. 99–125.
33. Rahmati, S.; Doherty, W.; Dubal, D.; Atanda, L.; Moghaddam, L.; Sonar, P.; Hessel, V.; Ostrikov, K. Pretreatment and fermentation of lignocellulosic biomass: Reaction mechanisms and process engineering. *React. Chem. Eng.* **2020**, *5*, 2017–2047. [CrossRef]
34. Oh, S.Y.; Yoo, D.I.; Shin, Y.; Kim, H.C.; Kim, H.Y.; Chung, Y.S.; Park, W.H.; Youk, J.H. Crystalline structure analysis of cellulose treated with sodium hydroxide and carbon dioxide by means of X-ray diffraction and FTIR spectroscopy. *Carbohydr. Res.* **2005**, *340*, 2376–2391. [CrossRef]
35. PÉrez, S.; Samain, D. Structure and Engineering of Celluloses. In *Advances in Carbohydrate Chemistry and Biochemistry*; Horton, D., Ed.; Academic Press: Cambridge, MA, USA, 2010; pp. 25–116.
36. Rongpipi, S.; Ye, D.; Gomez, E.D.; Gomez, E.W. Progress and Opportunities in the Characterization of Cellulose—An Important Regulator of Cell Wall Growth and Mechanics. *Front. Plant Sci.* **2019**, *9*, 1894. [CrossRef] [PubMed]
37. Oudiani, A.E.; Chaabouni, Y.; Msahli, S.; Sakli, F. Crystal transition from cellulose I to cellulose II in NaOH treated *Agave americana* L. fibre. *Carbohydr. Polym.* **2011**, *86*, 1221–1229. [CrossRef]
38. Coseri, S.; Biliuta, G.; Simionescu, B.C. Selective oxidation of cellulose, mediated by N-hydroxyphthalimide, under a metal-free environment. *Polym. Chem.* **2018**, *9*, 961–967. [CrossRef]
39. Saito, T.; Isogai, A. TEMPO-Mediated Oxidation of Native Cellulose. The Effect of Oxidation Conditions on Chemical and Crystal Structures of the Water-Insoluble Fractions. *Biomacromolecules* **2004**, *5*, 1983–1989. [CrossRef]
40. Chen, M.; Li, R.-M.; Runge, T.; Feng, J.; Feng, J.; Hu, S.; Shi, Q.-S. Solvent-Free Acetylation of Cellulose by 1-Ethyl-3-methylimidazolium Acetate-Catalyzed Transesterification. *ACS Sustain. Chem. Eng.* **2019**, *7*, 16971–16978. [CrossRef]
41. Yadav, P.; Chacko, S.; Kumar, G.; Ramapanicker, R.; Verma, V. Click chemistry route to covalently link cellulose and clay. *Cellulose* **2015**, *22*, 1615–1624. [CrossRef]
42. Guan, Q.-F.; Yang, H.-B.; Han, Z.-M.; Zhou, L.-C.; Zhu, Y.-B.; Ling, Z.-C.; Jiang, H.-B.; Wang, P.-F.; Ma, T.; Wu, H.-A.; et al. Lightweight, tough, and sustainable cellulose nanofiber-derived bulk structural materials with low thermal expansion coefficient. *Sci. Adv.* **2020**, *6*, eaaz1114. [CrossRef]
43. Antonietti, M. Sustainable Bulk Structural Material Engineered from Cellulose Nanofibers. *Matter* **2020**, *3*, 339–340. [CrossRef]
44. Chen, Y.; Dang, B.; Fu, J.; Wang, C.; Li, C.; Sun, Q.; Li, H. Cellulose-Based Hybrid Structural Material for Radiative Cooling. *Nano Lett.* **2021**, *21*, 397–404. [CrossRef]
45. Fan, J.; Zhang, S.; Li, F.; Shi, J. Cellulose-based sensors for metal ions detection. *Cellulose* **2020**, *27*, 5477–5507. [CrossRef]
46. Fan, J.; Zhang, S.; Li, F.; Yang, Y.; Du, M. Recent advances in cellulose-based membranes for their sensing applications. *Cellulose* **2020**, *27*, 9157–9179. [CrossRef] [PubMed]
47. Ummartyotin, S.; Manuspiya, H. A critical review on cellulose: From fundamental to an approach on sensor technology. *Renew. Sustain. Energy Rev.* **2015**, *41*, 402–412. [CrossRef]
48. Qiu, X.; Hu, S. "Smart" Materials Based on Cellulose: A Review of the Preparations, Properties, and Applications. *Materials* **2013**, *6*, 738–781. [CrossRef] [PubMed]
49. Wang, J.; He, J.; Ma, L.; Zhang, Y.; Shen, L.; Xiong, S.; Li, K.; Qu, M. Multifunctional conductive cellulose fabric with flexibility, superamphiphobicity and flame-retardancy for all-weather wearable smart electronic textiles and high-temperature warning device. *Chem. Eng. J.* **2020**, *390*, 124508. [CrossRef]

50. Sjöström, E. (Ed.) LIGNIN. In *Wood Chemistry: Fundamentals and Applications*; Academic Press: San Diego, CA, USA, 1993; Chapter 4, pp. 71–89.
51. Evstigneyev, E.I.; Shevchenko, S.M. Structure, chemical reactivity and solubility of lignin: A fresh look. *Wood Sci. Technol.* **2019**, *53*, 7–47. [CrossRef]
52. Cline, S.P.; Smith, P.M. Opportunities for lignin valorization: An exploratory process. *Energy Sustain. Soc.* **2017**, *7*, 26. [CrossRef]
53. LLP, K.S.I. *Lignin Market—Forecasts from 2020 to 2025*; Research and Markets: Dublin, Ireland, 2020.
54. Naomi, R.; Idrus, R.B.H.; Fauzi, M.B. Plant- vs. Bacterial-Derived Cellulose for Wound Healing: A Review. *Int. J. Environ. Res. Public Health* **2020**, *17*, 6803. [CrossRef]
55. Research, G.V. *Cellulose Fiber Market Size, Share & Trends Analysis by Product Type (Natural, Synthetic), by Application (Textile, Hygiene, Industrial), by Regions and Segment Forecasts, 2018—2025*; Grand View Research: San Francisco, CA, USA, 2016.
56. Nguyen, N.A.; Meek, K.M.; Bowland, C.C.; Barnes, S.H.; Naskar, A.K. An Acrylonitrile–Butadiene–Lignin Renewable Skin with Programmable and Switchable Electrical Conductivity for Stress/Strain-Sensing Applications. *Macromolecules* **2018**, *51*, 115–127. [CrossRef]
57. Glasser, W.G. About Making Lignin Great Again—Some Lessons from the Past. *Front. Chem.* **2019**, *7*, 565. [CrossRef]
58. Sezer, N.; Koç, M. A comprehensive review on the state-of-the-art of piezoelectric energy harvesting. *Nano Energy* **2021**, *80*, 105567. [CrossRef]
59. Zheng, Q.; Zhang, H.; Mi, H.; Cai, Z.; Ma, Z.; Gong, S. High-performance flexible piezoelectric nanogenerators consisting of porous cellulose nanofibril (CNF)/poly(dimethylsiloxane) (PDMS) aerogel films. *Nano Energy* **2016**, *26*, 504–512. [CrossRef]
60. Atalla, R.H.; Vanderhart, D.L. Native cellulose: A composite of two distinct crystalline forms. *Science* **1984**, *223*, 283–285. [CrossRef] [PubMed]
61. Yun, G.-Y.; Kim, J.-H.; Kim, J. Dielectric and polarization behaviour of cellulose electro-active paper (EAPap). *J. Phys. D Appl. Phys.* **2009**, *42*, 082003. [CrossRef]
62. Fukada, E. Piezoelectricity of Wood. *J. Phys. Soc. Jpn.* **1955**, *10*, 149–154. [CrossRef]
63. Gong, S.; Zhang, B.; Zhang, J.; Wang, Z.L.; Ren, K. Biocompatible Poly(lactic acid)-Based Hybrid Piezoelectric and Electret Nanogenerator for Electronic Skin Applications. *Adv. Funct. Mater.* **2020**, *30*, 1908724. [CrossRef]
64. Kalimuldina, G.; Turdakyn, N.; Abay, I.; Medeubayev, A.; Nurpeissova, A.; Adair, D.; Bakenov, Z. A Review of Piezoelectric PVDF Film by Electrospinning and Its Applications. *Sensors* **2020**, *20*, 5214. [CrossRef] [PubMed]
65. Song, J.; Zhao, G.; Li, B.; Wang, J. Design optimization of PVDF-based piezoelectric energy harvesters. *Heliyon* **2017**, *3*, e00377. [CrossRef]
66. Wang, J.; Carlos, C.; Zhang, Z.; Li, J.; Long, Y.; Yang, F.; Dong, Y.; Qiu, X.; Qian, Y.; Wang, X. Piezoelectric Nanocellulose Thin Film with Large-Scale Vertical Crystal Alignment. *ACS Appl. Mater. Interfaces* **2020**, *12*, 26399–26404. [CrossRef]
67. Li, J.; Kang, L.; Yu, Y.; Long, Y.; Jeffery, J.J.; Cai, W.; Wang, X. Study of long-term biocompatibility and bio-safety of implantable nanogenerators. *Nano Energy* **2018**, *51*, 728–735. [CrossRef]
68. Mahadeva, S.K.; Walus, K.; Stoeber, B. Piezoelectric Paper Fabricated via Nanostructured Barium Titanate Functionalization of Wood Cellulose Fibers. *ACS Appl. Mater. Interfaces* **2014**, *6*, 7547–7553. [CrossRef]
69. Csoka, L.; Hoeger, I.C.; Rojas, O.J.; Peszlen, I.; Pawlak, J.J.; Peralta, P.N. Piezoelectric Effect of Cellulose Nanocrystals Thin Films. *ACS Macro Lett.* **2012**, *1*, 867–870. [CrossRef]
70. Bairagi, S.; Ghosh, S.; Ali, S.W. A fully sustainable, self-poled, bio-waste based piezoelectric nanogenerator: Electricity generation from pomelo fruit membrane. *Sci. Rep.* **2020**, *10*, 12121. [CrossRef] [PubMed]
71. Sun, J.; Guo, H.; Schädli, G.N.; Tu, K.; Schär, S.; Schwarze, F.W.; Panzarasa, G.; Ribera, J.; Burgert, I. Enhanced mechanical energy conversion with selectively decayed wood. *Sci. Adv.* **2021**, *7*, eabd9138. [CrossRef]
72. Ram, F.; Radhakrishnan, S.; Ambone, T.; Shanmuganathan, K. Highly Flexible Mechanical Energy Harvester Based on Nylon 11 Ferroelectric Nanocomposites. *ACS Appl. Polym. Mater.* **2019**, *1*, 1998–2005. [CrossRef]
73. Zhu, Y.; Romain, C.; Williams, C.K. Sustainable polymers from renewable resources. *Nature* **2016**, *540*, 354–362. [CrossRef]
74. Drioli, E.; Brunetti, A.; Di Profio, G.; Barbieri, G. Process intensification strategies and membrane engineering. *Green Chem.* **2012**, *14*, 1561–1572. [CrossRef]
75. Meringolo, C.; Mastropietro, T.F.; Poerio, T.; Fontananova, E.; DE Filpo, G.; Curcio, E.; Di Profio, G. Tailoring PVDF Membranes Surface Topography and Hydrophobicity by a Sustainable Two-Steps Phase Separation Process. *ACS Sustain. Chem. Eng.* **2018**, *6*, 10069–10077. [CrossRef]
76. Oliver-Ortega, H.; Méndez, J.A.; Reixach, R.; Espinach, F.X.; Ardanuy, M.; Mutjé, P. Towards More Sustainable Material Formulations: A Comparative Assessment of PA11-SGW Flexural Performance versus Oil-Based Composites. *Polymers* **2018**, *10*, 440. [CrossRef]
77. Sessini, V.; Haseeb, B.; Boldizar, A.; Re, G.L. Sustainable pathway towards large scale melt processing of the new generation of renewable cellulose–polyamide composites. *RSC Adv.* **2021**, *11*, 637–656. [CrossRef]
78. Alam, M.M.; Mandal, D. Native Cellulose Microfiber-Based Hybrid Piezoelectric Generator for Mechanical Energy Harvesting Utility. *ACS Appl. Mater. Interfaces* **2016**, *8*, 1555–1558. [CrossRef]
79. Choi, H.Y.; Jeong, Y.G. Microstructures and piezoelectric performance of eco-friendly composite films based on nanocellulose and barium titanate nanoparticle. *Compos. Part B Eng.* **2019**, *168*, 58–65. [CrossRef]

80. Shi, K.; Huang, X.; Sun, B.; Wu, Z.; He, J.; Jiang, P. Cellulose/$BaTiO_3$ aerogel paper based flexible piezoelectric nanogenerators and the electric coupling with triboelectricity. *Nano Energy* **2019**, *57*, 450–458. [CrossRef]
81. Ponnamma, D.; Parangusan, H.; Tanvir, A.; AlMa'adeed, M.A.A. Smart and robust electrospun fabrics of piezoelectric polymer nanocomposite for self-powering electronic textiles. *Mater. Des.* **2019**, *184*, 108176. [CrossRef]
82. Li, M.; Jie, Y.; Shao, L.-H.; Guo, Y.; Cao, X.; Wang, N.; Wang, Z.L. All-in-one cellulose based hybrid tribo/piezoelectric nanogenerator. *Nano Res.* **2019**, *12*, 1831–1835. [CrossRef]
83. Pusty, M.; Shirage, P.M. Gold nanoparticle–cellulose/PDMS nanocomposite: A flexible dielectric material for harvesting mechanical energy. *RSC Adv.* **2020**, *10*, 10097–10112. [CrossRef]
84. Toroń, B.; Szperlich, P.; Nowak, M.; Stróż, D.; Rzychoń, T. Novel piezoelectric paper based on SbSI nanowires. *Cellulose* **2018**, *25*, 7–15. [CrossRef]
85. Fan, F.-R.; Tian, Z.-Q.; Wang, Z.L. Flexible triboelectric generator. *Nano Energy* **2012**, *1*, 328–334. [CrossRef]
86. Wang, Z.L. Triboelectric Nanogenerators as New Energy Technology for Self-Powered Systems and as Active Mechanical and Chemical Sensors. *ACS Nano* **2013**, *7*, 9533–9557. [CrossRef]
87. Kim, D.W.; Lee, J.H.; Kim, J.K.; Jeong, U. Material aspects of triboelectric energy generation and sensors. *NPG Asia Mater.* **2020**, *12*, 6. [CrossRef]
88. Song, G.; Kim, Y.; Yu, S.; Kim, M.-O.; Park, S.-H.; Cho, S.M.; Velusamy, D.B.; Cho, S.H.; Kim, K.L.; Kim, J.; et al. Molecularly Engineered Surface Triboelectric Nanogenerator by Self-Assembled Monolayers (METS). *Chem. Mater.* **2015**, *27*, 4749–4755. [CrossRef]
89. Wang, S.; Xie, Y.; Niu, S.; Lin, L.; Liu, C.; Zhou, Y.S.; Wang, Z.L. Maximum Surface Charge Density for Triboelectric Nanogenerators Achieved by Ionized-Air Injection: Methodology and Theoretical Understanding. *Adv. Mater.* **2014**, *26*, 6720–6728. [CrossRef] [PubMed]
90. Zhang, X.S.; Han, M.D.; Wang, R.X.; Meng, B.; Zhu, F.Y.; Sun, X.M.; Hu, W.; Wang, W.; Li, Z.H.; Zhang, H.X. High-performance triboelectric nanogenerator with enhanced energy density based on single-step fluorocarbon plasma treatment. *Nano Energy* **2014**, *4*, 123–131. [CrossRef]
91. Zhang, R.; Dahlström, C.; Zou, H.; Jonzon, J.; Hummelgård, M.; Örtegren, J.; Blomquist, N.; Yang, Y.; Andersson, H.; Olsen, M.; et al. Cellulose-Based Fully Green Triboelectric Nanogenerators with Output Power Density of 300 W m^{-2}. *Adv. Mater.* **2020**, *32*, 2002824. [CrossRef] [PubMed]
92. Yao, C.; Hernandez, A.; Yu, Y.; Cai, Z.; Wang, X. Triboelectric nanogenerators and power-boards from cellulose nanofibrils and recycled materials. *Nano Energy* **2016**, *30*, 103–108. [CrossRef]
93. Niu, S.; Wang, Z.L. Theoretical systems of triboelectric nanogenerators. *Nano Energy* **2015**, *14*, 161–192. [CrossRef]
94. Jakmuangpak, S.; Prada, T.; Mongkolthanaruk, W.; Harnchana, V.; Pinitsoontorn, S. Engineering Bacterial Cellulose Films by Nanocomposite Approach and Surface Modification for Biocompatible Triboelectric Nanogenerator. *ACS Appl. Electron. Mater.* **2020**, *2*, 2498–2506. [CrossRef]
95. Shao, Y.; Feng, C.P.; Deng, B.W.; Yin, B.; Yang, M.B. Facile method to enhance output performance of bacterial cellulose nanofiber based triboelectric nanogenerator by controlling micro-nano structure and dielectric constant. *Nano Energy* **2019**, *62*, 620–627. [CrossRef]
96. Nie, S.; Cai, C.; Lin, X.; Zhang, C.; Lu, Y.; Mo, J.; Wang, S. Chemically Functionalized Cellulose Nanofibrils for Improving Triboelectric Charge Density of a Triboelectric Nanogenerator. *ACS Sustain. Chem. Eng.* **2020**, *8*, 18678–18685. [CrossRef]
97. Zhang, L.; Liao, Y.; Wang, Y.; Zhang, S.; Yang, W.; Pan, X.; Wang, Z.L. Cellulose II Aerogel-Based Triboelectric Nanogenerator. *Adv. Funct. Mater.* **2020**, *30*, 2001763. [CrossRef]
98. Bao, Y.; Wang, R.; Lu, Y.; Wu, W. Lignin biopolymer based triboelectric nanogenerators. *APL Mater.* **2017**, *5*, 074109. [CrossRef]
99. Ramage, M.H.; Burridge, H.; Busse-Wicher, M.; Fereday, G.; Reynolds, T.; Shah, D.U.; Wu, G.; Yu, L.; Fleming, P.; Densley-Tingley, D.; et al. The wood from the trees: The use of timber in construction. *Renew. Sustain. Energy Rev.* **2017**, *68*, 333–359. [CrossRef]
100. Zhong, C. Industrial-Scale Production and Applications of Bacterial Cellulose. *Front. Bioeng. Biotechnol.* **2020**, *8*, 1425. [CrossRef] [PubMed]
101. Kim, D.; Jeon, S.-B.; Kim, J.Y.; Seol, M.-L.; Kim, S.O.; Choi, Y.-K. High-performance nanopattern triboelectric generator by block copolymer lithography. *Nano Energy* **2015**, *12*, 331–338. [CrossRef]
102. Zhang, F.; Li, B.; Zheng, J.; Xu, C. Facile Fabrication of Micro-Nano Structured Triboelectric Nanogenerator with High Electric Output. *Nanoscale Res. Lett.* **2015**, *10*, 298. [CrossRef]
103. Samejima, T.; Soh, Y.; Yano, T. Specific Surface Area and Specific Pore Volume Distribution of Tobacco. *Agric. Biol. Chem.* **1977**, *41*, 983–988. [CrossRef]
104. Zheng, Q.; Fang, L.; Guo, H.; Yang, K.; Cai, Z.; Meador, M.A.; Gong, S. Highly Porous Polymer Aerogel Film-Based Triboelectric Nanogenerators. *Adv. Funct. Mater.* **2018**, *28*, 1706365. [CrossRef]
105. Saadatnia, Z.; Mosanenzadeh, S.G.; Esmailzadeh, E.; Naguib, H.E. A High Performance Triboelectric Nanogenerator Using Porous Polyimide Aerogel Film. *Sci. Rep.* **2019**, *9*, 1370. [CrossRef]
106. Sun, J.-G.; Yang, T.N.; Kuo, I.-S.; Wu, J.-M.; Wang, C.-Y.; Chen, L.-J. A leaf-molded transparent triboelectric nanogenerator for smart multifunctional applications. *Nano Energy* **2017**, *32*, 180–186. [CrossRef]

107. Lee, K.; Mhin, S.; Han, H.; Kwon, O.; Kim, W.B.; Song, T.; Kang, S.; Kim, K.M. A high-performance PDMS-based triboelectric nanogenerator fabricated using surface-modified carbon nanotubes via pulsed laser ablation. *J. Mater. Chem. A* **2022**, *10*, 1299–1308. [CrossRef]
108. Xiao, X.; Lü, C.; Wang, G.; Xu, Y.; Wang, J.; Yang, H. Flexible triboelectric nanogenerator from micro-nano structured polydimethylsiloxane. *Chem. Res. Chin. Univ.* **2015**, *31*, 434–438. [CrossRef]
109. Kim, H.-J.; Yim, E.-C.; Kim, J.-H.; Kim, S.-J.; Park, J.-Y.; Oh, I.-K. Bacterial Nano-Cellulose Triboelectric Nanogenerator. *Nano Energy* **2017**, *33*, 130–137. [CrossRef]
110. Jie, Y.; Jia, X.; Zou, J.; Chen, Y.; Wang, N.; Wang, Z.L.; Cao, X. Natural Leaf Made Triboelectric Nanogenerator for Harvesting Environmental Mechanical Energy. *Adv. Energy Mater.* **2018**, *8*, 1703133. [CrossRef]
111. Feng, Y.; Zhang, L.; Zheng, Y.; Wang, D.; Zhou, F.; Liu, W. Leaves based triboelectric nanogenerator (TENG) and TENG tree for wind energy harvesting. *Nano Energy* **2019**, *55*, 260–268. [CrossRef]
112. Xiong, J.; Cui, P.; Chen, X.; Wang, J.; Parida, K.; Lin, M.F.; Lee, P.S. Skin-touch-actuated textile-based triboelectric nanogenerator with black phosphorus for durable biomechanical energy harvesting. *Nat. Commun.* **2018**, *9*, 4280. [CrossRef]
113. Yu, Z.; Wang, Y.; Zheng, J.; Xiang, Y.; Zhao, P.; Cui, J.; Zhou, H.; Li, D. Rapidly fabricated triboelectric nanogenerator employing insoluble and infusible biomass materials by fused deposition modeling. *Nano Energy* **2020**, *68*, 104382. [CrossRef]
114. Ramon, G.Z.; Feinberg, B.J.; Hoek, E.M.V. Membrane-based production of salinity-gradient power. *Energy Environ. Sci.* **2011**, *4*, 4423–4434. [CrossRef]
115. Pattle, R.E. Production of Electric Power by mixing Fresh and Salt Water in the Hydroelectric Pile. *Nature* **1954**, *174*, 660. [CrossRef]
116. Liu, X.; He, M.; Calvani, D.; Qi, H.; Gupta, K.B.S.S.; de Groot, H.J.; Sevink, G.A.; Buda, F.; Kaiser, U.; Schneider, G.F. Power generation by reverse electrodialysis in a single-layer nanoporous membrane made from core–rim polycyclic aromatic hydrocarbons. *Nat. Nanotechnol.* **2020**, *15*, 307–312. [CrossRef]
117. Wu, Q.; Wang, C.; Wang, R.; Chen, C.; Gao, J.; Dai, J.; Liu, D.; Lin, Z.; Hu, L. Salinity-Gradient Power Generation with Ionized Wood Membranes. *Adv. Energy Mater.* **2020**, *10*, 1902590. [CrossRef]
118. Moreno, J.; Grasman, S.; Van Engelen, R.; Nijmeijer, K. Upscaling Reverse Electrodialysis. *Environ. Sci. Technol.* **2018**, *52*, 10856–10863. [CrossRef]
119. Siria, A.; Bocquet, M.-L.; Bocquet, L. New avenues for the large-scale harvesting of blue energy. *Nat. Rev. Chem.* **2017**, *1*, 0091. [CrossRef]
120. Długołęcki, P.; Dąbrowska, J.; Nijmeijer, K.; Wessling, M. Ion conductive spacers for increased power generation in reverse electrodialysis. *J. Membr. Sci.* **2010**, *347*, 101–107. [CrossRef]
121. Ding, L.; Xiao, D.; Lu, Z.; Deng, J.; Wei, Y.; Caro, J.; Wang, H. Oppositely Charged Ti3C2Tx MXene Membranes with 2D Nanofluidic Channels for Osmotic Energy Harvesting. *Angew. Chem.* **2020**, *59*, 8720–8726. [CrossRef]
122. Pendse, A.; Cetindag, S.; Rehak, P.; Behura, S.; Gao, H.; Nguyen, N.H.L.; Wang, T.; Berry, V.; Král, P.; Shan, J.; et al. Highly Efficient Osmotic Energy Harvesting in Charged Boron-Nitride-Nanopore Membranes. *Adv. Funct. Mater.* **2021**, *31*, 2009586. [CrossRef]
123. Fu, Y.; Guo, X.; Wang, Y.; Wang, X.; Xue, J. An atomically-thin graphene reverse electrodialysis system for efficient energy harvesting from salinity gradient. *Nano Energy* **2019**, *57*, 783–790. [CrossRef]
124. Wu, Y.; Xin, W.; Kong, X.-Y.; Chen, J.; Qian, Y.; Sun, Y.; Zhao, X.; Chen, W.; Jiang, L.; Wen, L. Enhanced ion transport by graphene oxide/cellulose nanofibers assembled membranes for high-performance osmotic energy harvesting. *Mater. Horiz.* **2020**, *7*, 2702–2709. [CrossRef]
125. Beaumont, M.; Kondor, A.; Plappert, S.; Mitterer, C.; Opietnik, M.; Potthast, A.; Rosenau, T. Surface properties and porosity of highly porous, nanostructured cellulose II particles. *Cellulose* **2017**, *24*, 435–440. [CrossRef]
126. Dahlström, C.; Durán, V.L.; Keene, S.; Salleo, A.; Norgren, M.; Wågberg, L. Ion conductivity through TEMPO-mediated oxidated and periodate oxidated cellulose membranes. *Carbohydr. Polym.* **2020**, *233*, 115829. [CrossRef] [PubMed]
127. Muhmed, S.A.; Nor, N.A.M.; Jaafar, J.; Ismail, A.F.; Othman, M.H.D.; Rahman, M.A.; Aziz, F.; Yusof, N. Emerging chitosan and cellulose green materials for ion exchange membrane fuel cell: A review. *Energy Ecol. Environ.* **2020**, *5*, 85–107. [CrossRef]
128. Väisänen, S.; Pönni, R.; Hämäläinen, A.; Vuorinen, T. Quantification of accessible hydroxyl groups in cellulosic pulps by dynamic vapor sorption with deuterium exchange. *Cellulose* **2018**, *25*, 6923–6934. [CrossRef]
129. de Assis Filho, R.B.; de Araújo, C.M.B.; Baptisttella, A.M.S.; Batista, E.B.; Barata, R.A.; Ghislandi, M.G.; da Motta Sobrinho, M.A. Environmentally friendly route for graphene oxide production via electrochemical synthesis focused on the adsorptive removal of dyes from water. *Environ. Technol.* **2020**, *41*, 2771–2782. [CrossRef] [PubMed]
130. Pei, S.; Wei, Q.; Huang, K.; Cheng, H.-M.; Ren, W. Green synthesis of graphene oxide by seconds timescale water electrolytic oxidation. *Nat. Commun.* **2018**, *9*, 145. [CrossRef]
131. Chufa, B.M.; Gonfa, B.A.; Anshebo, T.Y.; Workneh, G.A. A Novel and Simplest Green Synthesis Method of Reduced Graphene Oxide Using Methanol Extracted *Vernonia Amygdalina*: Large-Scale Production. *Adv. Condens. Matter Phys.* **2021**, *2021*, 6681710.
132. Hummers, W.S.; Offeman, R.E. Preparation of Graphitic Oxide. *J. Am. Chem. Soc.* **1958**, *80*, 1339. [CrossRef]
133. Zaaba, N.I.; Foo, K.L.; Hashim, U.; Tan, S.J.; Liu, W.W.; Voon, C.H. Synthesis of Graphene Oxide using Modified Hummers Method: Solvent Influence. *Procedia Eng.* **2017**, *184*, 469–477. [CrossRef]
134. Smith, A.T.; LaChance, A.M.; Zeng, S.; Liu, B.; Sun, L. Synthesis, properties, and applications of graphene oxide/reduced graphene oxide and their nanocomposites. *Nano Mater. Sci.* **2019**, *1*, 31–47. [CrossRef]

135. Villafaña-López, L.; Reyes-Valadez, D.M.; González-Vargas, O.A.; Suárez-Toriello, V.A.; Jaime-Ferrer, J.S. Custom-Made Ion Exchange Membranes at Laboratory Scale for Reverse Electrodialysis. *Membranes* **2019**, *9*, 145. [CrossRef]
136. Wu, Z.; Ji, P.; Wang, B.; Sheng, N.; Zhang, M.; Chen, S.; Wang, H. Oppositely charged aligned bacterial cellulose biofilm with nanofluidic channels for osmotic energy harvesting. *Nano Energy* **2021**, *80*, 105554. [CrossRef]
137. Sheng, N.; Chen, S.; Zhang, M.; Wu, Z.; Liang, Q.; Ji, P.; Wang, H. TEMPO-Oxidized Bacterial Cellulose Nanofibers/Graphene Oxide Fibers for Osmotic Energy Conversion. *ACS Appl. Mater. Interfaces* **2021**, *13*, 22416–22425. [CrossRef] [PubMed]
138. Shi, Y.; Wang, Y.; Deng, Y.; Gao, H.; Lin, Z.; Zhu, W.; Ye, H. A novel self-powered wireless temperature sensor based on thermoelectric generators. *Energy Convers. Manag.* **2014**, *80*, 110–116. [CrossRef]
139. Mukaida, M.; Kirihara, K.; Horike, S.; Wei, Q. Stable organic thermoelectric devices for self-powered sensor applications. *J. Mater. Chem. A* **2020**, *8*, 22544–22556. [CrossRef]
140. Hewawasam, L.; Jayasena, A.; Afnan, M.; Ranasinghe, R.; Wijewardane, M. Waste heat recovery from thermo-electric generators (TEGs). *Energy Rep.* **2020**, *6*, 474–479. [CrossRef]
141. Hashim, H.T. Energy Harvesting from the Waste Heat of an Electrical Oven via Thermoelectric Generator. *J. Phys. Conf. Ser.* **2018**, *1032*, 012024. [CrossRef]
142. Lin, S.; Li, W.; Chen, Z.; Shen, J.; Ge, B.; Pei, Y. Tellurium as a high-performance elemental thermoelectric. *Nat. Commun.* **2016**, *7*, 10287. [CrossRef]
143. Zheng, Z.-H.; Shi, X.-L.; Ao, D.-W.; Liu, W.-D.; Li, M.; Kou, L.-Z.; Chen, Y.-X.; Li, F.; Wei, M.; Liang, G.-X.; et al. Harvesting waste heat with flexible Bi2Te3 thermoelectric thin film. *Nat. Sustain.* **2023**, *6*, 180–191. [CrossRef]
144. Zhao, X.; Han, W.; Jiang, Y.; Zhao, C.; Ji, X.; Kong, F.; Xu, W.; Zhang, X. A honeycomb-like paper-based thermoelectric generator based on a Bi2Te3/bacterial cellulose nanofiber coating. *Nanoscale* **2019**, *11*, 17725–17735. [CrossRef]
145. Zhao, X.; Zhao, C.; Jiang, Y.; Ji, X.; Kong, F.; Lin, T.; Shao, H.; Han, W. Flexible cellulose nanofiber/Bi2Te3 composite film for wearable thermoelectric devices. *J. Power Sources* **2020**, *479*, 229044. [CrossRef]
146. Ying, P.; He, R.; Mao, J.; Zhang, Q.; Reith, H.; Sui, J.; Ren, Z.; Nielsch, K.; Schierning, G. Towards tellurium-free thermoelectric modules for power generation from low-grade heat. *Nat. Commun.* **2021**, *12*, 1121. [CrossRef]
147. Xu, Y.; Ren, Z.; Ren, W.; Cao, G.; Deng, K.; Zhong, Y. Hydrothermal synthesis of single-crystalline Bi2Te3 nanoplates. *Mater. Lett.* **2008**, *62*, 4273–4276. [CrossRef]
148. Kim, J.-J.; Kim, S.-H.; Suh, S.-W.; Choe, D.-U.; Park, B.-K.; Lee, J.-R.; Lee, Y.-S. Hydrothermal synthesis of Bi2Te3 nanowires through the solid-state interdiffusion of Bi and Te atoms on the surface of Te nanowires. *J. Cryst. Growth* **2010**, *312*, 3410–3415. [CrossRef]
149. Fu, J.; Song, S.; Zhang, X.; Cao, F.; Zhou, L.; Li, X.; Zhang, H. Bi2Te3 nanoplates and nanoflowers: Synthesized by hydrothermal process and their enhanced thermoelectric properties. *CrystEngComm* **2012**, *14*, 2159–2165. [CrossRef]
150. Li, T.; Zhang, X.; Lacey, S.D.; Mi, R.; Zhao, X.; Jiang, F.; Song, J.; Liu, Z.; Chen, G.; Dai, J.; et al. Cellulose ionic conductors with high differential thermal voltage for low-grade heat harvesting. *Nat. Mater.* **2019**, *18*, 608–613. [CrossRef]
151. Kim, P.; Shi, L.; Majumdar, A.; McEuen, P.L. Thermal Transport Measurements of Individual Multiwalled Nanotubes. *Phys. Rev. Lett.* **2001**, *87*, 215502. [CrossRef] [PubMed]
152. Gnanaseelan, M.; Chen, Y.; Luo, J.; Krause, B.; Pionteck, J.; Pötschke, P.; Qi, H. Cellulose-carbon nanotube composite aerogels as novel thermoelectric materials. *Compos. Sci. Technol.* **2018**, *163*, 133–140. [CrossRef]
153. Abol-Fotouh, D.; Dörling, B.; Zapata-Arteaga, O.; Rodríguez-Martínez, X.; Gómez, A.; Reparaz, J.S.; Laromaine, A.; Roig, A.; Campoy-Quiles, M. Farming thermoelectric paper. *Energy Environ. Sci.* **2019**, *12*, 716–726. [CrossRef] [PubMed]
154. Kumanek, B.; Stando, G.; Wrobel, P.; Krzywiecki, M.; Janas, D. Thermoelectric properties of composite films from multi-walled carbon nanotubes and ethyl cellulose doped with heteroatoms. *Synth. Met.* **2019**, *257*, 116190. [CrossRef]
155. Culebras, M.; Ren, G.; O'Connell, S.; Vilatela, J.J.; Collins, M.N. Lignin Doped Carbon Nanotube Yarns for Improved Thermoelectric Efficiency. *Adv. Sustain. Syst.* **2020**, *4*, 2000147. [CrossRef]
156. Hu, J.; Li, R.; Zhang, K.; Meng, Y.; Wang, M.; Liu, Y. Extract nano cellulose from flax as thermoelectric enhancement material. *J. Phys. Conf. Ser.* **2021**, *1790*, 012087. [CrossRef]
157. Mardi, S.M.; Ambrogioni, R.; Reale, A. Developing printable thermoelectric materials based on graphene nanoplatelet/ethyl cellulose nanocomposites. *Mater. Res. Express* **2020**, *7*, 085101. [CrossRef]